Department of Physics and Astronomy

University of Heidelberg

Master thesis in Physics

submitted by

Fabian Lauble

born in Villingen-Schwenningen

2017

Practical Criterion for Single-Photon Entanglement at X-Ray Energies

This Master thesis has been carried out by

Fabian Lauble

at the

Max-Planck-Institut für Kernphysik

under the supervision of

Priv.-Doz. Dr. Jörg Evers

Practical Criterion for Single-Photon Entanglement at X-Ray Energies

The generation and verification of entanglement is one of the big remaining challenges in x-ray quantum optics. We generalize a criterion for two-mode entanglement based on a Bell inequality, which was put forward by Johansen. We show that the experimentally simple criterion detects entanglement even for arbitrary losses behind the source. Furthermore, a beamsplitter of arbitrary reflectivity can be used to generate two-mode entanglement from a single-photon input. We investigate a range of other interesting input states and find that states similar to the single-photon state produce entanglement as well. The criterion thus provides a robust and practical benchmark for both theoretical and experimental work on single-photon entanglement. By applying a post-selection scheme, we demonstrate the importance of two-photon events in experiments, even for very low event rates. The criterion's possible experimental implementation at x-ray energies, requiring only an interferometer and photodetectors, is discussed. We investigate Mössbauer nuclei in a thin-film cavity as an interferometer and derive a scheme to extract the first-order coherence $g^{(1)}$ from its Fano spectrum. Analyzing experimental data, we show that thin-film cavity systems are capable of sufficiently high coherence for the interferometry part of the criterion.

Praktikables Kriterium für Einzelphotonverschränkung bei Röntgenenergien

Die Erzeugung und Überprüfung von Verschränkung ist eines der großen verbleibenden Herausforderungen in der Röntgen-Quantenoptik. Wir generalisieren ein Kriterium für zwei-Moden-Verschränkung, basierend auf einer Bellungleichung und aufgestellt von Johansen. Wir zeigen, dass das experimentell einfach umzusetzende Kriterium sogar für beliebige Verluste hinter der Quelle Verschränkung anzeigt. Weiterhin zeigen wir, dass ein Strahlteiler von beliebiger Reflektivität benutzt werden kann, um die zwei-Moden-Verschränkung aus einem Einzelphotoneingang zu erzeugen. Wir untersuchen eine Reihe von interessanten Eingangszuständen und stellen fest, dass dem Einzelphotonzustand ähnliche Zustände ebenfalls Verschränkung erzeugen.Dadurch kann das Kriterium als robuster und praktikabler Maßstab sowohl für theoretische als auch experimentelle Arbeiten zur Einzelphotonverschränkung dienen. Mithilfe einer Postselektionsrechnung wird aufgezeigt, wie wichtig die Beachtung von zwei-Photonen-Ereignissen in Experimenten ist, selbst bei sehr niedrigen Zählraten. Die mögliche experimentelle Umsetzung des Kriteriums im Röntgenbereich mithilfe eines Interferometers und Photodetektoren wird diskutiert. Wir untersuchen Mößbauerkerne in einer Dünnschichtkavität als Interferometer und leiten ein Schema zur Extraktion der Kohärenz erster Ordnung, $g^{(1)}$, aus dem Fano-Spektrum ab. Mithilfe einer Analyse experimenteller Daten weisen wir nach, dass Dünnschichtkavitäten in der Lage sind, ausreichend hohe Kohärenz für den Interferometrie-Teil des Kriteriums zu erzeugen.

Bell's Theorem

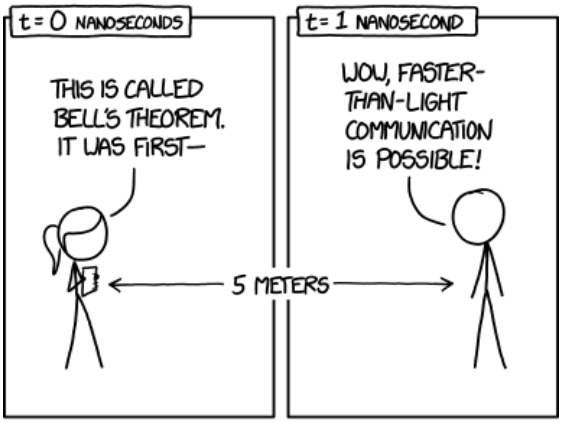

[1]

[1] https://xkcd.com/1591/ [Mun]

Contents

Chapter 1

Introduction

Quantum theory is so radically different from its predecessors that nowadays, every other physical theory is usually called 'classical physics'. While the theory is very successful in describing nature to great accuracy, the fundamental concepts did not sit well with many physicists. The most famous quantum skeptic was Albert Einstein, who himself had challenged the then-established notions of absolute time and space. He rejected the probabilistic interpretation of quantum theory, summarized in his famous quote "[God] doesn't throw dice" [EB72]. Einstein, Podolsky, and Rosen formulated the famous EPR thought experiment [EPR35], in which they considered a pair of entangled particles. They showed the incompatibility of QT with the classical notions of *realism* (i.e. that God doesn't throw dice) and *locality*, which is at the heart of classical field theory [Jac07]. EPR concluded that quantum theory is "incomplete", and demanded a modification to comply with local realism. Through the first decades of quantum theory, this discussion was metaphysical. Quantum theory continued to produce accurate descriptions of reality but was never modified to the satisfaction of EPR. But in 1964, John S. Bell [Bel64] showed that these classical notions were actually testable. He derived an inequality for theories satisfying both realism and locality and showed that the actual predictions were different from quantum theory. Thus, the demanded modification of quantum theory is impossible and quantum theory's agreement with experimental data suggested that local realism is false. Numerous experimental tests of Bell's inequality have been conducted, starting with Freedman and Clauser's first experiment in 1972 [FC72], and the evidence in favor of quantum theory is overwhelming [Gen05]. The foremost goal of subsequent experiments was to close 'loopholes', culminating in three recent refutations of local realism that are loophole-free [Hen+15][Giu+15][Sha+15].

Only a few years before quantum theory took its first steps, Wilhelm Conrad Röntgen [Rö98] investigated what we now call x-radiation. It exhibits remarkable attributes and facilitated valuable applications: because of their short wavelength, x-rays penetrate matter and thus enable doctors to look inside the human body [Bus02], material scientists to reveal the structure of crystals [War69], life

scientists to investigate macromolecules [Dre07] and quantum physicists to excite high-energy states in atoms, ions [BKS97] and nuclei [Mö58][HT99]. While Röntgen studied the radiation of x-ray tubes, today's scientists utilize the advantages of high-brilliance synchrotron [BEW05] or x-ray free-electron laser facilities [Emm+10][Alt+06], light sources with unprecedented coherence and intensity.
Compared to the ivory tower debate about locality and realism, x-ray science has been dedicated mostly to hands-on applications. But what might have been a discrepancy in the last century is a closing gap today. The emerging field of quantum information science [NC02] has shown that quantum entanglement can be a resource rather than a limitation, needed for the eagerly anticipated quantum computers [DiV95] and quantum cryptography devices [BB84][Gis+02]. On the other hand, the new x-ray light sources have enabled physicists to observe effects that previously have only been observed with visible light. These include spontaneous parametric down-conversion [EM71][Ada03][Tam+11][SH11][Shw+14], collective Lamb shift [Rö+10], x-ray control with light [Glo+10], x-ray–optical wave mixing [Glo+12], electromagnetically induced transparency in nuclei [Rö+12], atomic x-ray lasing [Roh+12][Yon+15], stimulated x-ray emmission [Bey+13], spontaneously generated coherences [Hee+13], slow light [Hee+15a] and x-ray ghost imaging [Pel+16].
In future quantum technology, entangled x-ray fields may play a significant role. X-ray photons suffer less dispersion than optical photons and can be narrowly focused due to their short wavelength. While they will not replace optical photons for all applications, they might serve as a backbone for long-distance quantum key distribution, utilizing the easy handling of optical photons and low dispersion of x-ray photons. Furthermore, x-ray photons facilitate applications that are simply not possible with optical photons. Ideas of this kind include the manipulation of long-lived nuclear states for storing and releasing energy [Car+01] or macroscopic quantum entanglement [LKP16].
Quantum entanglement has not yet been observed at x-ray energies. This is mainly due to the still inferior light sources compared to visible-light optics. There are, however, proposals for entanglement generation: Spontaneous parametric down-conversion, the most important source for entangled photon pairs in the optical regime [Shi03], is also possible at multi-keV energies [EM71][Ada03]. The generation of polarization-entangled x-ray photon has been proposed by Shwartz et al. [SH11]. However, x-ray PDC suffers from very small event rates of about one pair in 10 seconds when driven with a third-generation synchrotron with ~ 10^{12} photons per pulse [Ada03].
Pálffy, Keitel, and Evers [PKE09] and Liao and Pálffy [LP14] propose the generation of single-photon entanglement by magnetic switching of a Mössbauer nuclear forward scattering sample [Shv+96]. The synchrotron source has on average far less than one resonant photon per pulse, giving rise to a single excitation of the nuclear ensemble [HT99]. This limitation (or differentiator) is the main reason for the interest in single-photon entanglement in the field of nuclear optics. For entanglement verification, both references suggest the violation of a single-

photon Bell inequality put forward by Lee and Kim, using only a Mach-Zehnder interferometer [LK00].
The Lee–Kim proposal also awakened interest in the context of Mössbauer nuclei in thin-film cavities, a system that has recently been interpreted as an interferometer [Hee+15b] in the framework of a quantum optical model by Heeg and Evers [HE13]. The prompted research to implement interferometer criterion in these cavity systems [Zha16] lead to the original project of this thesis.
Our examination of Ref. [LK00] uncovered that it cannot be used for entanglement detection, which is discussed in section 3.5. The research for a different, experimentally simple entanglement criterion led to the paper by Johansen [Joh96], who introduced a criterion for two-mode states, based on a Bell inequality. It is violated by a single-photon entangled state and can be measured using both an interferometry and a coincidence setup. It builds directly upon the work of Tan, Holland, and Walls [THW90]. It is simple compared to a proper test of the underlying Bell inequality but requires a coincidence experiment as distinct from the Lee–Kim proposal. Johansen [Joh96] showed that the idealized case of single-photon entanglement, generated by a single-photon state impinging on a lossless, balanced beamsplitter meets the criterion.

In order to be applied as a practical entanglement test, Johansen's criterion has to be extended to non-ideal parameters. The goal of this thesis is to generalize Johansen's result to lossy optical instruments, a non-balanced beamsplitter and deviations from the single-photon input.
We start with an introduction to entanglement and Bell's inequality and present the derivation of the Johansen criterion in chapter 2. Chapter 3 presents our main results: We consider losses behind the source and a general, i.e. non-balanced beamsplitter as a source for entanglement. Both imperfections do not impair the criterion's power to detect entanglement. Then, a wide range of states for the beamsplitter input is presented. The portion similar to the single-photon state illustrates the robustness of the criterion. The other portion illustrates the differences to both classical states and entangled states that do not meet Johansen's criterion.
In nuclear excitations, the low rate of resonant photons leads to the assumption of single-photon phenomena. We will discuss differences between weak classical states and a single-photon state in the context of entanglement using a post-selection scheme in section 3.4. In chapter 4, we apply the results to instrumentation and entanglement proposals for the x-ray regime. After summarizing the requirements, we discuss the feasibility of entanglement detection and possible entanglement generation techniques. In section 4.3, we turn to the system of Mössbauer nuclei embedded in thin-film cavities. We assess its ability to implement the interferometer part of the Johansen criterion by deriving a relation between the Fano line shape visibility and the coherence of first order. Using experimental data, we show that nuclei in cavities are capable of meeting the interferometry requirement of the Johansen criterion.

Chapter 2

Theoretic Background

In this chapter, we will introduce the concept of quantum entanglement and its relation to Bell's inequality, before discussing the special case of single-photon entanglement. The main part of the chapter will present the derivation of Johansen's entanglement criterion [Joh96], following the original derivation closely.

Notation

The Dirac Bra–Ket notation ($\langle \text{bra}|\,, |\text{ket}\rangle$) will be used throughout to denote pure states and we will use density matrices ρ to describe mixed states [GT09]. We will specialize to optical systems, so the creation and annihilation operators $a^\dagger$, a, $b^\dagger$, b, ... for light modes $a, b, \ldots$ will arise. They satisfy the standard commutation relation [WM94]

$$\left[a_k, a_l^\dagger\right] = \delta_{k\,l}\,.$$

Since we will discuss entanglement of two seperate subsystems, the letters A, $a, \alpha, \aleph$ will usually refer to the subsystem of 'Alice'; letters B, $b, \beta, \beth$ to Bob's subsystem. Exceptions are $|\alpha\rangle$ for a coherent state and $\mathscr{B}$ for the Bell quantity.

2.1 Entanglement

While entanglement is arguably quantum theory's most distinct feature, it is not easy to detect. Even deciding whether a given quantum state ρ is entangled isn't trivial and remains an open problem for Hilbert spaces of larger dimension [GT09].
The formal definition of entanglement for a pure state $|\psi\rangle$ on a Hilbert space $\mathscr{H} = \mathscr{H}_\mathrm{A} \otimes \mathscr{H}_\mathrm{B}$ is

$$|\psi\rangle \text{ is entangled} :\Longleftrightarrow |\psi\rangle \text{ is } \textit{not} \text{ separable}, \tag{2.1}$$

$$|\psi\rangle \text{ is separable} :\Longleftrightarrow |\psi\rangle = |\phi\rangle_\mathrm{A} \otimes |\zeta\rangle_\mathrm{B} = |\phi\rangle_\mathrm{A}\,|\zeta\rangle_\mathrm{B}\,, \tag{2.2}$$

i.e. we can find states $|\phi\rangle_\mathrm{A}$, $|\zeta\rangle_\mathrm{B}$ on the subspaces $\mathscr{H}_\mathrm{A}$, $\mathscr{H}_\mathrm{B}$ to write $|\psi\rangle$ as a *product state*.
For mixed states, represented by density matrices ρ, the definition is similar:

$$\rho \text{ is entangled } :\Longleftrightarrow \rho \text{ is } \textit{not} \text{ separable}, \tag{2.3}$$

$$\rho \text{ is separable } :\Longleftrightarrow \rho = \sum_i p_i \, \rho_\mathrm{A}^i \otimes \rho_\mathrm{B}^i \,, \tag{2.4}$$

where the p_i are positive probabilities that sum up to one and all $\rho_\mathrm{A/B}^i$ are density matrices on the subspaces. Separable, mixed states are not only product states but also statistical mixtures of product states. This second definition introduces classical correlations, which are different from quantum correlations. For example, consider having two lollipops, one green and one red. Alice and Bob want one each, preferably the green one. To be fair, we toss a (fair) coin. If we do not know the outcome of the coin toss, this can be represented by the density matrix

$$\rho_\text{mixed} = \left(|\mathrm{r}\rangle_\mathrm{A}\,|\mathrm{g}\rangle_\mathrm{B}\,\langle\mathrm{r}|_\mathrm{A}\,\langle\mathrm{g}|_\mathrm{B} + |\mathrm{g}\rangle_\mathrm{A}\,|\mathrm{r}\rangle_\mathrm{B}\,\langle\mathrm{g}|_\mathrm{A}\,\langle\mathrm{r}|_\mathrm{B}\right)\frac{1}{2} \mathrel{\hat{=}} \frac{1}{2}\begin{pmatrix}0&0&0&0\\0&1&0&0\\0&0&1&0\\0&0&0&0\end{pmatrix}. \tag{2.5}$$

The vector $|\mathrm{r}\rangle_\mathrm{A}\,|\mathrm{r}\rangle_\mathrm{B}$ corresponds to $(1,\,0,\,0,\,0)^\mathrm{T}$ and so on. The corresponting matrix element, the upper left one, is zero, because we do not have two red lollipops. The states shows (anti-)correlation because Alice and Bob never both get the same color, but is separable by the above definition. Of course, it is objectively determined who got which lollipop. The uncertainty is just because of not knowing the outcome of the coin toss. Thus, this state is equivalent to a probability vector, which is the main diagonal. In contrast to this, consider an entangled state

$$|\psi_+\rangle = \left(|\mathrm{r}\rangle_\mathrm{A}\,|\mathrm{g}\rangle_\mathrm{B} + |\mathrm{g}\rangle_\mathrm{A}\,|\mathrm{r}\rangle_\mathrm{B}\right)\frac{1}{\sqrt{2}}\,, \tag{2.6}$$

$$\rho_\text{entangled} = |\psi_+\rangle\,\langle\psi_+| \mathrel{\hat{=}} \frac{1}{2}\begin{pmatrix}0&0&0&0\\0&1&1&0\\0&1&1&0\\0&0&0&0\end{pmatrix}. \tag{2.7}$$

While this state's entanglement can be checked because of the small Hilbert space, the *separability problem* is, in general, a hard problem in quantum information theory. It is therefore natural to seek a measure of entanglement. Furthermore, we also want to detect entanglement in the laboratory, where the density matrix is often not directly accessible. *Bell's inequality* provides both a theoretical and experimental test of entanglement: If the state violates a Bell inequality, it is certainly entangled. In the laboratory, no further assumptions, like on Hilbert space dimension, have to be made.

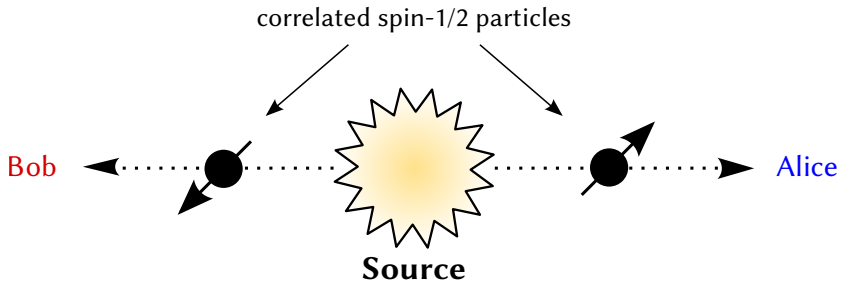

Figure 2.1: A Bell experiment with two spin-1/2 particles, two parties Alice and Bob, and two possible outcomes per measurement. Figure based on [Mik07].

2.2 Bell's Inequality

A Bell experiment is a test of fundamental principles of nature. It tests whether a local hidden-variable (LHV) theory can describe nature, which was demanded by EPR. Quantum theory is at odds with locality because of instantaneous wave-function collapse and with realism because of its intrinsic probabilistic nature [Per02].
Assuming a local hidden variable model, Bell proved that certain correlations of spatially distant measurements cannot exceed a certain bound, *Bell's inequality*. Quantum theory exceeds this bound for certain states, and thus follows Bell's Theorem: QT is incompatible with local hidden variables. A very accessible explanation can be found in Peres [Per02, p. 160]. Many Bell experiments have been performed to decide whether local realism or quantum theory is correct, and the matter was decided in favor of quantum mechanics [Gen05].
There are several versions of Bell's inequality. The best-known kind of Bell experiments is depicted in figure 2.1. A source emits a system that is decomposed into 2 subsystems, for example a pair of spin-$\frac{1}{2}$ particles. Alice and Bob perform one out of 2 measurements (spin-measurement along two different axes, given by angles θ_a, θ_b) and each measurement can give 2 different results (spin up or spin down). The best-known Bell inequality for this setup is the CHSH–Bell inequality [Cla+69]. It considers a correlation quantity $E(\theta_a, \theta_b)$ for correlations of the measurements outcomes of Alice and Bob. The inequality arises when we add this quantity for different measurement settings θ_a, θ_b:

$$\mathscr{B} := E(\theta_a, \theta_b) + E(\theta_a, \theta'_b) + E(\theta'_a, \theta_b) - E(\theta'_a, \theta'_b) \,. \tag{2.8}$$

$\mathscr{B}$ can be bound be local hidden variables to obtain the Bell–CHSH inequality

$$\mathscr{B} \overset{\text{LHV}}{\leq} 2 \,. \tag{2.9}$$

But $\mathscr{B}$ can exceed this value according to quantum theory. QT's upper limit was derived by Cirel'son [Cir80]:

$$\mathscr{B} \overset{\text{QT}}{\leq} 2\sqrt{2} \approx 2.83. \tag{2.10}$$

A violation of Bell's inequality implies that the state was *entangled*. Therefore, Bell inequalities where amongst the first methods to quantifiy and determine entanglement. A seperable, i.e. not entangled state will certainly not violate a Bell inequality, but a given entangled state does not necessarily violate it. We therefore cannot deduce anything from not violating a Bell inequality. Today, implications for quantum applications are an equally important reason to study Bell violations: They are linked to the security of quantum cryptography protocols and have additional fundamental implications [GT09].
Let us note here for clarification, that the violation of the principle of locality does not mean that faster-than-light communication is possible [PT04]. Only after communicating the recorded results of the distant parties do the correlations exceed classical bounds. Alice's *choices* cannot influence Bob's measurement outcomes and thus a 'Bell telephone' cannot be constructed.
A Bell inequality is certainly a proper tool for an entanglement criterion. Before introducing a Bell inequality suitable for single-photon entanglement, we will discuss this special case.

2.3 Single-Photon Entanglement

One might wonder how single-photon entanglement can exist. Entanglement with two *parties* involved two *particles* in the CHSH experiment. While often, the number of parties (Alice, Bob, ...) is equal to the number of particles, this is is not necessarily the case.
Consider two (e.g. spatial) modes a and b, and a single photon that is in a superposition of being in one and the other mode:

$$|\psi_+\rangle = \frac{1}{\sqrt{2}} \left(|1\rangle_a |0\rangle_b + |0\rangle_a |1\rangle_b \right) , \tag{2.11}$$

where $|n\rangle_x$ is the n-photon Fock state [WM94] in mode x and the single-photon state in mode a is $|1\rangle_a = a^\dagger |\text{vac}\rangle$. This state is entangled like eq. (2.6) according to the seperability criterion and called a single-photon entangled state. It is a bipartite state since two modes are entangled.
In the case of two entangled spin-1/2 particles, both parties have one particle to perform measurements on and the two particles are usually said to be entangled. Therefore, the concept of single-photon entanglement can be puzzling. The state (2.11) is clearly not separable and thus an entangled state. In that sense, quantum theory does not care about the physical realizations of the state; if the pure state cannot be written as a product state, the state is entangled. A helpful intuition may be that the two (spatial) *modes* are entangled *by* the single photon.
In 1989, Oliver and Stroud [OS89] proposed that a single photon can violate a Bell inequality. Probably independently, Tan, Holland, and Walls [THW90] showed that single-photon entanglement violates a Bell inequality put forward by Reid and Walls [RW86]. Refs. [THW90] and [TWC91] stirred much debate: Since a single photon is destroyed upon detection, a Bell experiment's measurements in

differing bases have to be realized with additional photons, in this case through the local oscillators of the homodyne detection scheme. However, these additional photons raise the question whether the anticipated non-local effect can be attributed to a single-photon or rather to a multi-photon effect [San92a] [TWC92] [Gra88][San92b] [Har94] [GHZ95] [Per95]. The most simple and striking argument in defense for single-photon entanglement may be Peres's: Every measurement apparatus contains particles and the photons of the local oscillators are just particles of the respective measurement apparatus [Per95]. The generation of the local oscillators may of course raise practical implications, if the two 'local' oscillators are generated from the same light source and thus might carry correlations themselves. There is continued interest in single-photon entangled states. Lombardi et al. [Lom+02] have realized quantum teleportation with the scheme by [LK00][1]and Knill, Laflamme, and Milburn [KLM01]. Hessmo et al. [Hes+04] have verified the entanglement proposed by [TWC91] and Hardy [Har94]. More recently, following the suggestion of [JW11], Fuwa et al. [Fuw+15] have violated a steering inequality, which is connected to the EPR thought experiment.
Instead of violating a fundamental inequality, we will now derive the result by Johansen [Joh96], which uses the Bell inequality of Reid and Walls and the results of [THW90] to obtain an entanglement criterion. Such a criterion can help to verify the entanglement of a source's states before tackling a fundamental criterion. Since it is derived from a Bell inequality, these states *will* violate the proper Bell test, in contrast to arbitrary entangled states.

2.4 Deriving the Entanglement Criterion

Building on the work of Tan, Holland, and Walls, Johansen put forward a scheme to measure whether states violate Bell's inequality using only an interferometer and a coincidence counter [Joh96]. We will derive the criterion, following Johansen's paper. Some steps were shown by [THW90]. We will start from the Bell inequality by Reid and Walls [RW86].

2.4.1 Bell Inequality for Phase-Sensitive Measurements

Reid and Walls's Bell experiment is depicted in figure 2.2. Consider a general light source of two single-mode output beams a, b, that are spatially separated. To measure the relative phase, the detection of both beams is of homodyne fashion: The beams are superposed with local oscillator (LO) modes ℓ_a and ℓ_b, represented by coherent states $|\alpha_{\mathrm{LO}}\rangle$ and $|\beta_{\mathrm{LO}}\rangle$, using balanced (50/50) beamsplitters. In this thesis, a beamsplitter will always use the phase choice such that the balanced

[1]Lee and Kim's paper contains two parts; one about quantum teleportation, and one about a single-particle Bell inequality. Sec. 3.5 is about the latter.

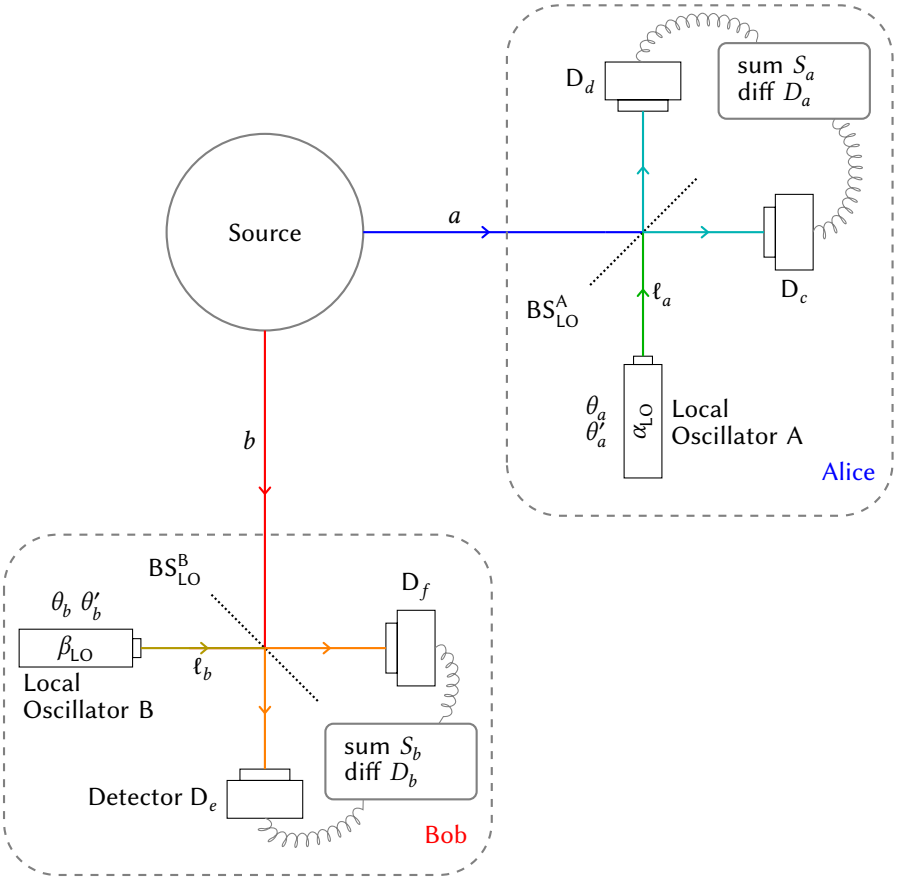

Figure 2.2: Bell experiment using homodyne detection. The source emits light in two spatial modes. Alice and Bob can perform two measurements by setting one of two particular phases θ_i, θ'_i of the local oscillators. In contrast to the CHSH case in Fig. 2.1, the measurements yield continuous values. The local observables S_i and D_i are combined to correlation quantities $E(\theta_a, \theta_b)$, which form the Bell quantity $\mathscr{B}$.

beamsplitter is described by relating the annihilation operators like

$$\begin{pmatrix} c \\ d \end{pmatrix} = \frac{1}{\sqrt{2}} \begin{pmatrix} 1 & \mathrm{i} \\ \mathrm{i} & 1 \end{pmatrix} \begin{pmatrix} a \\ \ell_a \end{pmatrix}, \tag{2.12}$$

so that the transmitted beam does not get phase shifted. A non-50/50 beamsplitter with real transmittance amplitude t and real reflectance amplitude r with $t^2 + r^2 = 1$ is in this convention modelled with

$$\begin{pmatrix} c \\ d \end{pmatrix} = \begin{pmatrix} t & \mathrm{i}r \\ \mathrm{i}r & t \end{pmatrix} \begin{pmatrix} a \\ \ell_a \end{pmatrix}. \tag{2.13}$$

The homodyne detection is crucial for this setup to measure phases and to perform measurements at both local labs, even when the source emits only one photon in total.

The two detectors at each lab can measure not only time-averaged intensities but count rates for coincidence measurement. We will use the quantum theoretic terms $c^\dagger c$, $d^\dagger d$, $e^\dagger e$ and $f^\dagger f$ for the count rates to simplify notation. The derivation of the Bell inequality does however not use the quantum properties and is demonstrated in [RW86] with count rates.

We consider the local observables sum and difference of the two detector rates

$$S_a := c^\dagger c + d^\dagger d = a^\dagger a + \ell_a^\dagger \ell_a \,, \tag{2.14}$$

$$S_b := e^\dagger e + f^\dagger f = b^\dagger b + \ell_b^\dagger \ell_b \,, \tag{2.15}$$

$$D_a := c^\dagger c - d^\dagger d = \mathrm{i}\left(a^\dagger \ell_a - a \ell_a^\dagger\right) \,, \tag{2.16}$$

$$D_b := e^\dagger e - f^\dagger f = \mathrm{i}\left(b^\dagger \ell_b - b \ell_b^\dagger\right) \,, \tag{2.17}$$

where we used the beamsplitter relations to obtain the right-hand side expressions. We combine them into the the correlation function or 'modulation depth'

$$E(\theta_a, \theta_b) := \frac{\langle D_a D_b \rangle}{\langle S_a S_b \rangle} \,, \tag{2.18}$$

which depends on the phases θ_a, θ_b of *both* local oscillators: $\alpha_{\mathrm{LO}} = |\alpha_{\mathrm{LO}}| \mathrm{e}^{\mathrm{i}\theta_a}$ (analogous for θ_b). Unlike the correlation function in the discussed Bell-CHSH-Experiment [Cla+69], (2.18) can assume continuous values instead of ±1, but $|E| \leq 1$ holds as well. We define the analogue quantity

$$\mathscr{B} = E(\theta_a, \theta_b) + E(\theta_a, \theta_b') + E(\theta_a', \theta_b) - E(\theta_a', \theta_b') \,, \tag{2.19}$$

and assuming a local hidden-variable theory, one can derive an analogue Bell inequality [RW86]:

$$\mathscr{B} \overset{\mathrm{LHV}}{\leq} 2 \,. \tag{2.20}$$

Quantum theory allows again violation of this inequality up to the same Cirel'son bound [Cir80] [RW86]

$$\mathscr{B} \overset{\mathrm{QT}}{\leq} 2\sqrt{2} \approx 2.83 \,. \tag{2.21}$$

2.4.2 Eliminating the Measurement Parameters

In order to get an entanglement criterion from this Bell inequality, we need to eliminate the measurement settings. We do this by choosing the LO amplitudes α_{LO} and β_{LO}, including the phases θ_a, θ_b optimally. The goal is to find an expression that can be measured by simpler experiments than the homodyne measurement and still provide information on whether the state would exhibit Bell-violating behavior
First, we express E as a function of $a, a^\dagger, b, b^\dagger, \alpha_{\mathrm{LO}}$ and β_{LO}:

$$\begin{aligned}
\langle S_a S_b \rangle &= \left\langle \left(a^\dagger a + \ell_a^\dagger \ell_a\right)\left(b^\dagger b + \ell_b^\dagger \ell_b\right)\right\rangle \\
&= \left\langle a^\dagger a\, b^\dagger b\right\rangle + \left\langle a^\dagger a\right\rangle |\beta_{\mathrm{LO}}|^2 + \left\langle b^\dagger b\right\rangle |\alpha_{\mathrm{LO}}|^2 + |\alpha_{\mathrm{LO}}|^2 |\beta_{\mathrm{LO}}|^2 \qquad (2.22)\\
\langle D_a D_b \rangle &= \left\langle \mathrm{i}\left(a^\dagger \ell_a - a\ell_a^\dagger\right)\mathrm{i}\left(b^\dagger \ell_b - b\ell_b^\dagger\right)\right\rangle \\
&= \left\langle a^\dagger b\right\rangle \alpha_{\mathrm{LO}}\beta_{\mathrm{LO}}^* + \left\langle ab^\dagger\right\rangle \alpha_{\mathrm{LO}}^*\beta_{\mathrm{LO}} \\
&\quad - \langle ab\rangle \alpha_{\mathrm{LO}}^*\beta_{\mathrm{LO}}^* - \left\langle a^\dagger b^\dagger\right\rangle \alpha_{\mathrm{LO}}\beta_{\mathrm{LO}} \\
&= \left|\left\langle a^\dagger b\right\rangle \alpha_{\mathrm{LO}}\beta_{\mathrm{LO}}\right| 2\cos\left(\arg\left[\left\langle a^\dagger b\right\rangle\right] + (\theta_a - \theta_b)\right) \\
&\quad - \left|\langle ab\rangle \alpha_{\mathrm{LO}}\beta_{\mathrm{LO}}\right| 2\cos\left(\arg\left[\langle ab\rangle\right] - (\theta_a + \theta_b)\right) \qquad (2.23)
\end{aligned}$$

We combine these expressions to E and arrange it in one θ_i-independent part and one part independent of the magnitudes of the local oscillators:

$$E(\theta_a, \theta_b) = \mathscr{E}\left(|\alpha_{\mathrm{LO}}|, |\beta_{\mathrm{LO}}|\right) \times \epsilon(\theta_a, \theta_b)\,, \qquad (2.24)$$

$$\mathscr{E} = \frac{2\left|\alpha_{\mathrm{LO}}\beta_{\mathrm{LO}}\right|}{\langle a^\dagger a\, b^\dagger b\rangle + \langle a^\dagger a\rangle |\beta_{\mathrm{LO}}|^2 + \langle b^\dagger b\rangle |\alpha_{\mathrm{LO}}|^2 + |\alpha_{\mathrm{LO}}\beta_{\mathrm{LO}}|^2}\,, \qquad (2.25)$$

$$\begin{aligned}
\epsilon &= \left|\langle a^\dagger b\rangle\right| \cos\left(\arg\left[\left\langle a^\dagger b\right\rangle\right] + (\theta_a - \theta_b)\right) \\
&\quad - \left|\langle ab\rangle\right| \cos\left(\arg\left[\langle ab\rangle\right] - (\theta_a + \theta_b)\right)\,. \qquad (2.26)
\end{aligned}$$

In order to find the best measurement settings for violation of 2.20, we need to maximize $\mathscr{E}$ (2.25). To that end, we substitute $|\alpha_{\mathrm{LO}}| = \sqrt{xy}$, $|\beta_{\mathrm{LO}}| = \sqrt{xy^{-1}}$ and arrive at

$$\mathscr{E} = \frac{2}{\langle a^\dagger a\, b^\dagger b\rangle \frac{1}{x} + \langle a^\dagger a\rangle \frac{1}{y} + \langle b^\dagger b\rangle\, y + x}\,. \qquad (2.27)$$

To maximize $\mathscr{E}$, the denominator has to be minimized. Differentiating with respect to x and y and setting to zero yields

$$x = \left|\alpha_{\mathrm{LO}}\beta_{\mathrm{LO}}\right| = \sqrt{\left\langle a^\dagger a\, b^\dagger b\right\rangle}\,, \qquad (2.28)$$

$$y = \left|\frac{\alpha_{\mathrm{LO}}}{\beta_{\mathrm{LO}}}\right| = \sqrt{\frac{\langle a^\dagger a\rangle}{\langle b^\dagger b\rangle}}\,. \qquad (2.29)$$

Thus, if the magnitudes of the LO-amplitudes are chosen in this optimal way, $\mathscr{E}$ becomes

$$\mathscr{E} = \frac{1}{\sqrt{\langle a^\dagger a\, b^\dagger b\rangle} + \sqrt{\langle a^\dagger a\rangle \langle b^\dagger b\rangle}} \,. \tag{2.30}$$

Thus, we can write

$$\begin{aligned} E(\theta_a, \theta_b) = C_1 \cos\left(\theta_a - \theta_b + \arg[\langle a^\dagger b\rangle]\right) \\ + C_2 \cos\left(\theta_a + \theta_b - \arg[\langle ab\rangle]\right) \,, \end{aligned} \tag{2.31}$$

with

$$C_1 = \frac{\left|\langle a^\dagger b\rangle\right|}{\sqrt{\langle a^\dagger a\, b^\dagger b\rangle} + \sqrt{\langle a^\dagger a\rangle \langle b^\dagger b\rangle}} \quad \text{and} \tag{2.32}$$

$$C_2 = \frac{\left|\langle ab\rangle\right|}{\sqrt{\langle a^\dagger a\, b^\dagger b\rangle} + \sqrt{\langle a^\dagger a\rangle \langle b^\dagger b\rangle}} \,. \tag{2.33}$$

In order to violate Bell's inequality $\mathscr{B} \leq 2$, the LO-phases $\theta_a, \theta_a', \theta_b, \theta_b'$ have to be chosen in a suitable way, depending on the expectation values above. We now want to further eliminate these variables by assuming they are chosen optimally. We define $\xi_1 = -\arg[\langle a^\dagger b\rangle] - \pi/2$ and $\xi_2 = \arg[\langle ab\rangle] - \pi/2$ and set $\partial\mathscr{B}/\partial\theta_i = 0$ to find the extrema. If we use three out of four such conditions, [THW90] showed that the measurement phases have to be chosen as follows:

$$\theta_a = \frac{1}{2}(\xi_1 + \xi_2) \,, \qquad \theta_a' = \frac{1}{2}(\xi_1 + \xi_2) - \frac{\pi}{2} \,, \tag{2.34}$$

$$\theta_b = \frac{1}{2}(\xi_1 - \xi_2) - \zeta \,, \qquad \theta_b' = \frac{1}{2}(\xi_1 - \xi_2) + \zeta \,. \tag{2.35}$$

Here, ζ is a free parameter because one degree of freedom is still left. Then, one can write

$$\mathscr{B}(\zeta) = 2\sqrt{2}\,\sqrt{C_1^2 + C_2^2}\,\sin(\zeta - \zeta_0) \,, \tag{2.36}$$

$$\text{with} \quad \tan\zeta_0 = \frac{C_1 + C_2}{C_1 - C_2} \,. \tag{2.37}$$

Since $|\sin| \leq 1$, it is necessary for the violation of Bell's inequality that $C_1^2 + C_2^2 > \frac{1}{2}$. If ζ is chosen optimally, for example $\zeta = \zeta_0 + \frac{\pi}{2}$, Bell's inequality reduces to a condition on the expectation values:

$$\begin{aligned} \mathscr{B} &= 2\sqrt{2}\,\sqrt{C_1^2 + C_2^2} \\ &= 2\sqrt{2}\,\frac{\sqrt{\left|\langle a^\dagger b\rangle\right|^2 + \left|\langle ab\rangle\right|^2}}{\sqrt{\langle a^\dagger a\, b^\dagger b\rangle} + \sqrt{\langle a^\dagger a\rangle \langle b^\dagger b\rangle}} \overset{\text{LHV}}{\leq} 2 \,. \end{aligned} \tag{2.38}$$

The measurement parameters were chosen optimally for given expectation values $\langle a^\dagger a\, b^\dagger b\rangle$, $\langle a^\dagger a\rangle$, ... Experimentally, these parameters would need to be measured to optimize the Bell test. This choice allowed us to derive a condition on the entanglement of the bipartite state that is independent from the particular measurement. In the following, we will transfer this condition to a simpler measurement setup.

2.4.3 The Johansen Criterion

The measurement-independent Bell condition is again an inequality $\mathscr{B} \leq 2$. The idea is now to drop a term of $\mathscr{B}$, introducing a lower bound $\mathscr{B}' \leq \mathscr{B}$. We drop the $\langle ab\rangle$-part and define

$$\mathscr{B}' := 2\sqrt{2}\frac{\left|\langle a^\dagger b\rangle\right|}{\sqrt{\langle a^\dagger a\, b^\dagger b\rangle} + \sqrt{\langle a^\dagger a\rangle \langle b^\dagger b\rangle}} \,. \tag{2.39}$$

Since $\mathscr{B}' \leq \mathscr{B}$,

$$\mathscr{B}' \overset{\text{LHV}}{\leq} 2 \,, \tag{2.40}$$

so violation of $\mathscr{B}' \leq 2$ implies violation of the 'full' inequality $\mathscr{B} \leq 2$, but not vice versa. In that sense, it is weaker. We hope that $\mathscr{B}'$ is large 'enough' for some states and we will see shortly that it is not only sufficient, but just as good as the full inequality for our main interest, the single-photon entangled state. From now on, $\mathscr{B}$ and $\mathscr{B}'$ denote the quantities as defined in (2.38) and (2.39), independent of measurement choices.
We would not gain anything by the Johansen criterion if $\mathscr{B}'$ could only be measured in a Bell test. But fortunately, it depends only on expectation values that can be found in the (two-mode, equal-time) first and second order coherence functions

$$g^{(1)} = \frac{\langle a^\dagger b\rangle}{\sqrt{\langle a^\dagger a\rangle \langle b^\dagger b\rangle}} \,, \tag{2.41}$$

$$g^{(2)} = \frac{\langle a^\dagger a\, b^\dagger b\rangle}{\langle a^\dagger a\rangle \langle b^\dagger b\rangle} \,. \tag{2.42}$$

We can actually express $\mathscr{B}'$ in terms of the coherence functions:

$$\mathscr{B}' = 2\sqrt{2}\,\frac{\left|g^{(1)}\right|}{1 + \sqrt{g^{(2)}}} \,. \tag{2.43}$$

These quantities can be measured in a much simpler setup than the homodyne Bell setup with which we started. $|g^{(1)}|$ can be measured by superposing the two beams on a suitable beamsplitter and measuring the interference visibility, as in figure 2.4. $g^{(2)}$ can be measured with one detector in each beam, measuring

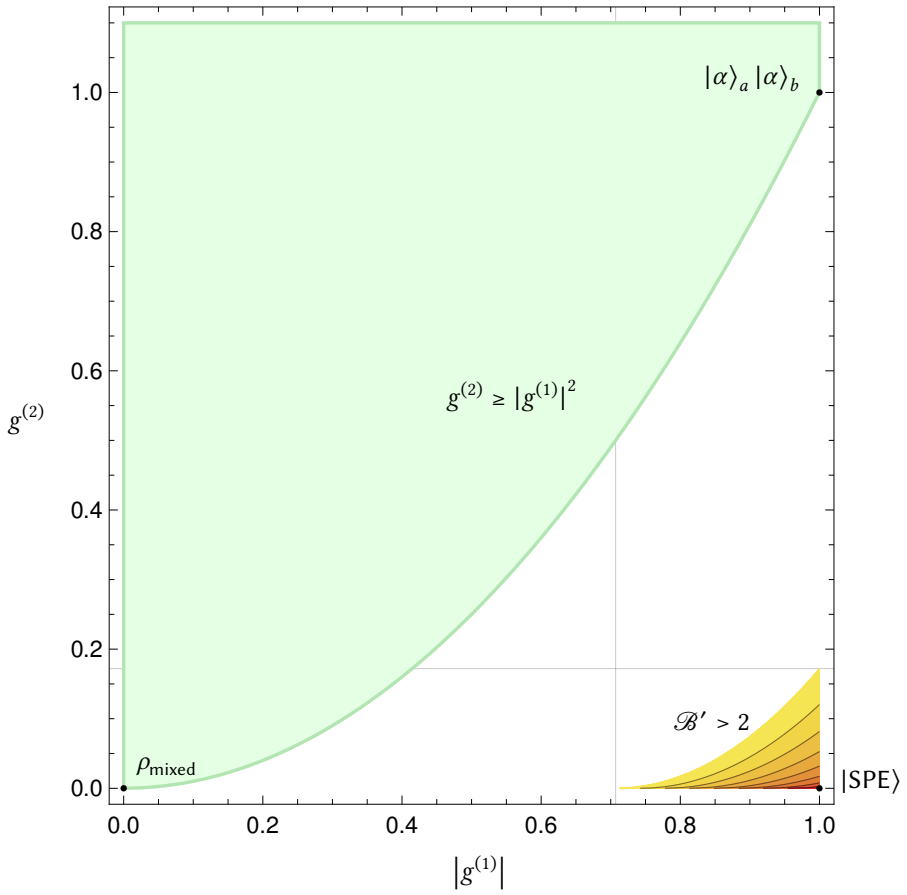

Figure 2.3: The Johansen entanglement criterion, where $\mathscr{B}' > 2$ indicates entanglement, in yellow–orange, in terms of the two-mode coherence functions $g^{(1)}$ and $g^{(2)}$, as definded in (2.41) and (2.42). Contour lines at $\mathscr{B}' = 2, 2.1, \ldots, 2.8$. The region for $\mathscr{B}' < 2$ is not plotted for clarity. Gray lines indicate the minimum requirements for $|g^{(1)}|$ and $g^{(2)}$ at ~ 0.707 and ~ 0.172, respectively. $\mathscr{B}'$ is maximal $(2\sqrt{2})$ at the lower right corner $(1, 1)$, which corresponds to the single-photon entangled state $|\text{SPE}\rangle$. The single-photon seperable mixed state ρ_{mixed} (2.54) is at $(0, 0)$, a two-mode separable coherent state $|\alpha\rangle_a |\alpha\rangle_b$ at $(1, 1)$. This state can be produced by illuminating a beamsplitter with a single coherent beam (see Chp. 3). For comparison, the condition $g^{(2)} \geq |g^{(1)}|^2$ from classical electrodynamics is shown in light green. As expected, all combinations of $|g^{(1)}|$ and $g^{(2)}$ which are allowed by cED do not satisfy the Johansen criterion.

coincidence, see figure 2.5. The normalizing factors $\langle a^\dagger a\rangle$ and $\langle b^\dagger b\rangle$ of $g^{(2)}$ can also be measured in the coincidence setup.
To violate $\mathscr{B}' \leq 2$ in a series of measurements with these simple setups implies that the measured state would violate a Bell inequality in the actual, complicated Bell experiment as in [THW90]. This may seem paradox. But we needed quantum theoretic calculations to arrive at this result, so no fundamental question may be answered by the simple coincidence and interference measurements.
However, these measurements enable us to detect certain Bell-violating, and thus entangled, states, assuming Quantum Theory is correct. The dependence of $\mathscr{B}'$ on the coherence functions is depicted in Fig. 2.3. For two arbitrary light modes a, b, $|g^{(1)}| \leq 1$ and $g^{(2)} \geq 0$. Classical light, i.e. classical electrodynamics, allows only

$$\left|g^{(1)}\right|^2 \leq g^{(2)} \tag{2.44}$$

because of the Cauchy–Schwarz inequality [Joh96] [TG65]. The $\mathscr{B}'$ inequality is harder to violate than the cED inequality. This illustrates that the class of local hidden variable theories is not equivalent to pre-quantum theories, but more general.
From Eq. (2.43) follow inequalities for $g^{(1)}$ and $g^{(2)}$ due to the general bounds of the coherence functions:

$$\left|g^{(1)}\right| \leq \frac{1}{\sqrt{2}} \approx 0.707 \,, \tag{2.45}$$

$$g^{(2)} \geq \left(\sqrt{2}-1\right)^2 \approx 0.172 \,. \tag{2.46}$$

These two inequalities are *necessary* for $\mathscr{B}' \overset{\text{LHV}}{\leq} 2$, but not sufficient.

Coherence $g^{(1)}$ and Interference Visibility

The relation between interference visibility and coherence of first order, $g^{(1)}$, can be found in textbooks on quantum optics [WM94]. We derive the standard case here because we will need to modify it later, when investigating interference in Fano line shapes in section 4.3.
Interference visibility quantifies the contrast of an interference fringe pattern, e.g. on a screen behind a double-slit. It also occurs in a Mach-Zehnder interferometer (Fig. 2.4), when measuring the intensity at one output port, e.g. at detector D_c, for varying phase shifts $\Delta\phi$, e.g. by inserting wave plates in the two arms. The visibility is defined as

$$\mathrm{VIS} = \frac{I_{\max} - I_{\min}}{I_{\max} + I_{\min}} \,, \tag{2.47}$$

where $I_{\max}$ [$I_{\min}$] is the intensity at the maximum [minimum] of the interference pattern. For a Mach-Zehnder interferometer with two modes a and b, output

mode c can be can be determined by the beamsplitter relation, analogue to (2.13). Without inserting wave plates, the intensity is given by

$$\begin{aligned} I_c = \left\langle c^\dagger c \right\rangle &= \left\langle (ta + \mathrm{i}rb)^\dagger (ta + \mathrm{i}rb) \right\rangle \\ &= t^2 \langle a^\dagger a \rangle + r^2 \langle b^\dagger b \rangle + \mathrm{i}tr \langle a^\dagger b \rangle - \mathrm{i}tr \langle a b^\dagger \rangle \\ &= t^2 \langle a^\dagger a \rangle + r^2 \langle b^\dagger b \rangle + 2tr \left| \langle a^\dagger b \rangle \right| \cos \Delta\phi \,, \end{aligned} \tag{2.48}$$

where $\Delta\phi = \arg[\langle a^\dagger b \rangle] + \pi \,/\, 2$ is the total relative phase between the interfering modes. If additional phase shifts ϕ_a and ϕ_b are introduced by inserting wave plates,

$$\Delta\phi = \phi_a - \phi_b + \arg[\langle a^\dagger b \rangle] + \frac{\pi}{2} \,. \tag{2.49}$$

Then, $I_{\max}\,[I_{\min}]$ corresponds to a relative phase of $\Delta\phi = 0\,[\Delta\phi = \pi]$, the phases with $\cos = 1\,[\cos = -1]$. This yields for the visibility

$$\begin{aligned} \mathrm{VIS} &= \frac{2tr \left| \langle a^\dagger b \rangle \right|}{t^2 \langle a^\dagger a \rangle + r^2 \langle b^\dagger b \rangle} \\ &= \frac{\left| \langle a^\dagger b \rangle \right|}{\sqrt{\langle a^\dagger a \rangle \langle b^\dagger b \rangle}} \;\; \frac{2tr\sqrt{\langle a^\dagger a \rangle \langle b^\dagger b \rangle}}{t^2 \langle a^\dagger a \rangle + r^2 \langle b^\dagger b \rangle} \\ &= \left| g^{(1)} \right| \;\; \frac{2tr\sqrt{\langle a^\dagger a \rangle \langle b^\dagger b \rangle}}{t^2 \langle a^\dagger a \rangle + r^2 \langle b^\dagger b \rangle} \,. \end{aligned} \tag{2.50}$$

For a balanced beamsplitter $r^2 = t^2 = 1 \,/\, 2$, one obtains

$$\begin{aligned} \mathrm{VIS} &= \left| g^{(1)} \right| \;\; \frac{2\sqrt{\langle a^\dagger a \rangle \langle b^\dagger b \rangle}}{\langle a^\dagger a \rangle + \langle b^\dagger b \rangle} \\ &= \left| g^{(1)} \right| \chi \,, \end{aligned} \tag{2.51}$$

with $\chi \leq 1$ and $\chi = 1$ for $\langle a^\dagger a \rangle = \langle b^\dagger b \rangle$. Thus, a balanced beamsplitter does not give the maximum visibility for imbalanced beams. However, if we choose the beamsplitter parameters r, t as

$$\begin{aligned} t^2 = \frac{\langle b^\dagger b \rangle}{\langle a^\dagger a \rangle + \langle b^\dagger b \rangle} \,, \quad r^2 = \frac{\langle a^\dagger a \rangle}{\langle a^\dagger a \rangle + \langle b^\dagger b \rangle} \,, \\ \mathrm{VIS} \longrightarrow \left| g^{(1)} \right| \quad \text{even for } \chi \neq 1 \,. \end{aligned} \tag{2.52}$$

Experimentally, one can vary the reflectivity until the interference visibility is maximal.

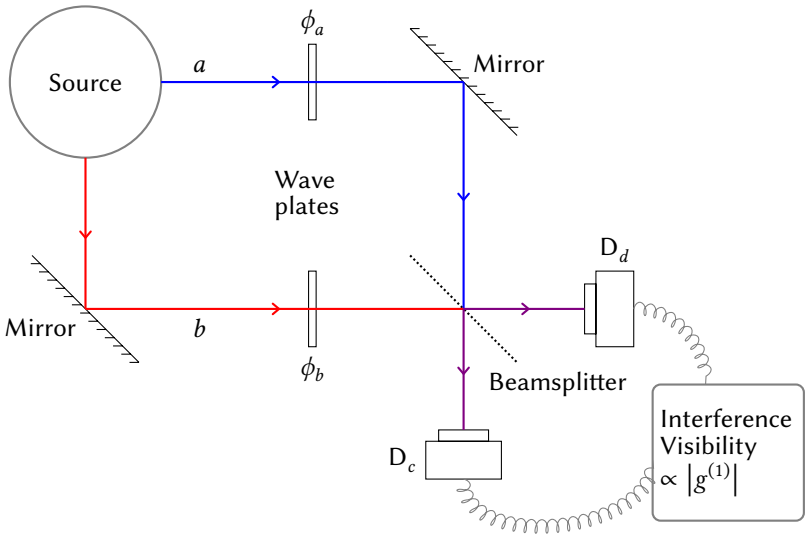

Figure 2.4: $g^{(1)}$ measurement in a Mach-Zehnder interferometer: The two beams are guided by mirrors, phase-shifted by wave plates and recombinded with a beamsplitter BS. By varying the relative phase $\Delta\phi$, an interference pattern can be recorded, using only one of the detectors. From the visibility of the interference pattern VIS = $(I_{max} - I_{min}) \nearrow (I_{max} + I_{min})$, the coherence $|g^{(1)}|$ can be derived. Generally, VIS $\leq |g^{(1)}|$.

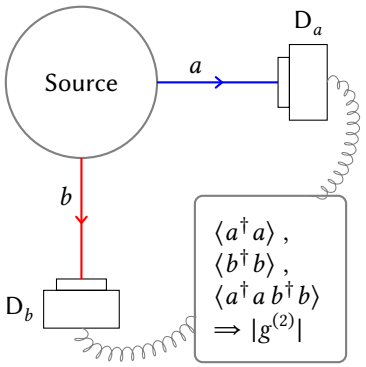

Figure 2.5: $g^{(2)}$ measurement via coincidence counting: An event is recorded only when both detectors click in the same time-window: $\langle a^\dagger a\, b^\dagger b \rangle$. The normalizations $\langle a^\dagger a \rangle$ and $\langle b^\dagger b \rangle$ can also be measured in this setup.

2.5 Evaluating the Inequality for Some States

Let us now look at some examples to illustrate which states meet the Johansen criterion and which do not.

Single-Photon Entangled State

Let the state of the light source be the single-photon entangled state

$$\begin{aligned} |\mathrm{SPE}\rangle = |\psi_\phi\rangle &= \frac{1}{\sqrt{2}}\left(|1\,0\rangle + \mathrm{e}^{\mathrm{i}\phi}\,|0\,1\rangle\right) \\ &= \frac{1}{\sqrt{2}}\left(|1\rangle_a\,|0\rangle_b + \mathrm{e}^{\mathrm{i}\phi}\,|0\rangle_a\,|1\rangle_b\right)\,, \end{aligned} \tag{2.53}$$

where $|n\rangle_i$ denotes the n-photon Fock state in the mode i and ϕ is an arbitrary phase. Then, $\langle a^\dagger a\, b^\dagger b\rangle = 0, \langle a^\dagger a\rangle = \langle b^\dagger b\rangle = |\langle a^\dagger b\rangle| = 1/2$ and therefore $\mathscr{B}' = 2\sqrt{2} > 2$. In terms of coherence functions, $|g^{(1)}| = 1, |g^{(2)}| = 0$. This is the maximal violation, even of the 'full' inequality $\mathscr{B} \leq 2$. It is independent of the relative phase ϕ.

Single-Photon Mixed state

However, if the source emits a classical mixture of '1 photon in A and none in B' and '1 photon in B and none in A', for example by tossing a coin to determine the direction of the photon, the state is given by the density matrix

$$\rho_{\mathrm{mixed}} = \frac{1}{2}\left(|1\,0\rangle\langle 1\,0| + |0\,1\rangle\langle 0\,1|\right) = \frac{1}{2}\begin{pmatrix} 0 & 0 & 0 & 0 \\ 0 & 1 & 0 & 0 \\ 0 & 0 & 1 & 0 \\ 0 & 0 & 0 & 0 \end{pmatrix}. \tag{2.54}$$

Again, $g^{(2)} = 0$. But this state does not exhibit any interference so $\langle a^\dagger b\rangle = 0 = g^{(1)}$, thus also $\mathscr{B}'$ vanishes, hence $\mathscr{B}' \leq 2$ is satisfied. This is expected since this fully mixed state is not entangled (see sec. 2.1).

Two-Photon state

The difference between the full $\mathscr{B}$ inequality and the Johansen criterion $\mathscr{B}'$ can be illustrated with the superposition of vacuum with the two-photon state

$$|2\gamma\rangle = s\,|1\,1\rangle + \sqrt{1-s^2}\;|0\,0\rangle\;. \tag{2.55}$$

This state is similar to the output of a parametric down-converter, which is discussed in [THW90] for this Bell inequality. For (2.55), $\langle a^\dagger b\rangle$ vanishes for all s, such that

$$\mathscr{B}' = 0 \tag{2.56}$$

and the Johansen criterion cannot detect entanglement. But the expectation value $\langle ab \rangle$ from $\mathscr{B}$, which was dropped in the derivation of $\mathscr{B}'$, is $\langle ab \rangle = s\sqrt{1-s^2}$. The coincidence is $\langle a^\dagger a\, b^\dagger b \rangle = s^2$ and the count rates yield $\langle a^\dagger a \rangle = \langle b^\dagger b \rangle = s^2$. Thus,

$$\begin{aligned} \mathscr{B} &= 2\sqrt{2}\,\frac{s\sqrt{1-s^2}}{s+s^2}\,, \\ \mathscr{B} &> 2 \quad \text{for } 0 < s < 1/3\,, \end{aligned} \tag{2.57}$$

so the state is entangled at least for $0 < s < 1/3$. This is one example for an entangled state the Johansen criterion cannot detect. Since not every entangled state violates a given Bell inequality, there are even entangled states that violate neither the $\mathscr{B}$ nor the $\mathscr{B}'$ inequality.

We showed in the previous sections how an entanglement criterion can be derived from a Bell inequality. Figure 2.6 shows the derivation in a flow-chart form. Starting with a complicated experiment involving local oscillators, the criterion can be checked in two simple experiments: coincidence and interferometry.
We gave a prototype example for an entangled state that is detected by the criterion: the ideal single-photon entangled state. As pointed out by e.g. [Joh96] [TWC91], such a state may be generated by a single-photon in one mode that impinges on a balanced beamsplitter. We will now turn to such a source of entanglement but generalize to a lossy, imbalanced beamsplitter.

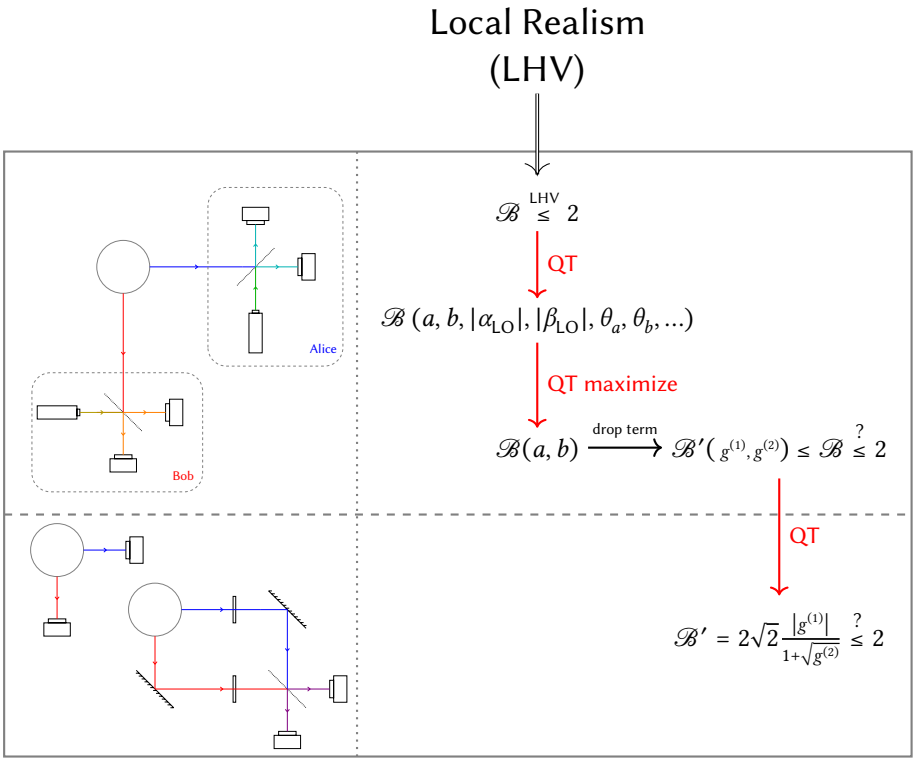

Figure 2.6: Overview of the inequalities used in this work. Starting from Local Realism in the form of Local Hidden Variable Models, one can derive the Bell inequality $\mathscr{B} \leq 2$ for the homodyne detection experiment in the first row. Quantum theory gives an expression for $\mathscr{B}$, depending on measurement parameters and properties of the source. Using this expression, we optimized the parameters of measurement, namely local oscillator parameters $|\alpha_{\text{LO}}|, |\beta_{\text{LO}}|, \theta_a, \theta'_a, \theta_b, \theta'_b$, arriving in the second row. Thus, only the properties of the source (a, b) remain. $\mathscr{B}'$ follows from $\mathscr{B}$ by dropping a positive term and is thus strictly smaller than $\mathscr{B}$. Then, we expressed $\mathscr{B}'$ in terms of quantities, that are accessible in simpler experiments, namely coincidence counting and interferometry. Thus, we arrived at the third row, at Johansen's criterion. Since we used quantum theory, a violation of,$bp \leq 2$ does not refute Local Realism. Rather, an entangled states is detected. One would need to perform the homodyne Bell experiment (first row and Fig. 2.2) to refute LHV theories.

Chapter 3

A Practical Criterion

In the following chapter, we will investigate the Johansen criterion and its practicality concerning non-ideal parameters. Specifically, we will show that a lossy, imbalanced beamsplitter can be used just as well as a balanced, lossless beamsplitter as an entanglement source. We will derive the criterion for the input mode of the beamsplitter and show an intuitive representation in photon statistics. We will see that not only the single-photon input can produce Johansen-criterion-entanglement.
In the last section (3.5), we will make a short detour and discuss a different proposal for a single-photon Bell inequality, put forward by Lee and Kim [LK00].

We now want to consider a source consisting of a beamsplitter, illuminated by a single mode of light. This is motivated by the fact that the single-photon entangled state (2.53) can be produced by a single-photon Fock state $|1\rangle_u$ at the input port u of a balanced beamsplitter (and vacuum at the other input port). The source beamsplitter is defined with the input port u, empty port v and output ports a', b' as

$$\begin{pmatrix} a' \\ b' \end{pmatrix} = \begin{pmatrix} א & \mathrm{i}\,ב \\ \mathrm{i}ב & א \end{pmatrix} \begin{pmatrix} u \\ v \end{pmatrix} \tag{3.1}$$

$$\Rightarrow \begin{pmatrix} u \\ v \end{pmatrix} = \begin{pmatrix} א & -\mathrm{i}\,ב \\ -\mathrm{i}ב & א \end{pmatrix} \begin{pmatrix} a' \\ b' \end{pmatrix}, \tag{3.2}$$

where the real parameters $א^2 + ב^2 = 1$ (the Hebrew letters Alef and Bet, respectively). In the lossless case, $a' = a$ and $b' = b$. Losses will be introduced shortly.
Using (3.2) for the mode u, we can write a single-photon input:

$$|1\rangle_u = u^\dagger |\mathrm{vac}\rangle \tag{3.3}$$

$$= (אa - \mathrm{i}\,ב b)^\dagger |\mathrm{vac}\rangle \tag{3.4}$$

$$= א |1\rangle_a |0\rangle_b + \mathrm{i}\,ב |0\rangle_a |1\rangle_b \ , \tag{3.5}$$

which, for a balanced beamsplitter ($א = ב = 1/\sqrt{2}$), gives the single-photon entangled state 2.53 with phase $\phi = \pi/2$. Irrespective of the phase, this state violates

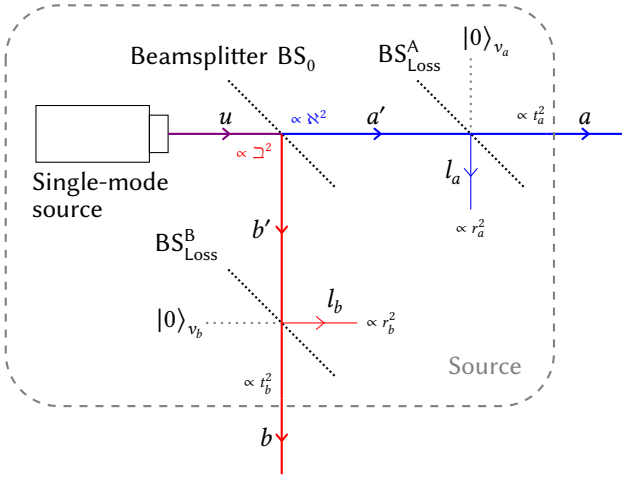

Figure 3.1: A single-mode source and a beamsplitter can act as a source for two-mode entanglement. In order to gain a practical criterion, we consider the general case of an imbalanced beamsplitter and losses thereafter, again modelled by beamsplitters. The first beamsplitter splits the single mode u (v is empty) into modes a' and b' with relative intensities $\aleph^2$ and $\beth^2$. The fictitious beamsplitters introduce losses, producing the actual modes a and b. The loss-beamsplitters have transmittivity t_a^2 and t_b^2 and also have vacuum at the other input ports.

the inequality $\mathscr{B}' \leq 2$ maximally with $\mathscr{B}' = 2\sqrt{2}$, and thus $\mathscr{B} = 2\sqrt{2}$. Thus, an ideal beamsplitter reduces the problem of entanglement generation to finding a single-photon source. We will now investigate whether this also holds for non-ideal beamsplitters and non-ideal single-photon sources, which is important for applications.

3.1 Lossy, Imbalanced Beamsplitter Source

We model losses after the initial beamsplitter with additional, fictitious beamsplitters as depicted in Fig. 3.1. The modes directly after the initial beamsplitter are a' and b' and the modes after the loss beamsplitters are called a and b, as they exit the source. The loss beamsplitter in the A path has the nomenclature: Input port a', empty input port v_a, main output port a, and loss output port l_a. The loss is parametrized by the real transmittance amplitude t_a (and reflectivity amplitude r_a). In the B path, the names are analogous. The beamsplitter relation is

$$\begin{pmatrix} a \\ l_a \end{pmatrix} = \begin{pmatrix} t_a & \mathrm{i}r_a \\ \mathrm{i}r_a & t_a \end{pmatrix} \begin{pmatrix} a' \\ v_a \end{pmatrix}. \tag{3.6}$$

The beamsplitter approach preserves the total photon number and the operator commutation relations. We lose photons because we omit the modes l_a and l_b 'downstream' and only consider a and b.

3.2 Criterion for the Initial Mode

In order to determine the degree of violation for various input states and beamsplitter parameters, we express $\mathscr{B}(a, a^\dagger, b, b^\dagger)$, using the beamsplitter relations, as $\mathscr{B}(u, u^\dagger, \aleph, t_a, t_b)$. The other parameters are fixed by conditions such as $\aleph^2 + \beth^2 = 1$. We do this for the full $\mathscr{B}$ quantitiy, because it is independent from the $\mathscr{B} \longrightarrow \mathscr{B}'$ derivation. We will get expressions for both $\mathscr{B}$ and $\mathscr{B}'$ for the case of a beamsplitter source.

We need to expand the two-mode expectation values on the right-hand side of eq. (2.38) using the beamsplitter relations. First, the modes a and b will be written as linear combinations of the pre-loss modes a' and v_a (v for vacuum) (and b' and v_b respectively). This represents the loss beamsplitters. Then, the modes a' and b' will be written in linear combinations of u and v, arising from the main beamsplitter (as in eq. 3.1). Since the ports v, v_a and v_b are vacuum ports, i.e. they are not illuminated by light, expectations values of the form $\langle \dots v_b \rangle$ or $\langle v_b^\dagger \dots \rangle$ will vanish because $v_b \left|0\right\rangle_{v_b} = 0$. Only terms such as $vv^\dagger = v^\dagger v + 1$ would contribute, but since all expectation values in $\mathscr{B}$ are normal-ordered, such terms do not arise. The calculation for the expectation value $\langle a^\dagger b \rangle$ will be demonstrated in detail:

$$
\begin{aligned}
\langle a^\dagger b \rangle &= \left\langle (t_a a' + \mathrm{i} r_a v_a)^\dagger \, (t_b b' + \mathrm{i} r_b v_b) \right\rangle \\
&= \left\langle \left(t_a a'^\dagger - \mathrm{i} r_a v_a^\dagger \right) \left(t_b b' + \mathrm{i} r_b v_b \right) \right\rangle \\
&= t_a t_b \langle a'^\dagger b' \rangle + \mathrm{i} t_a r_b \underbrace{\langle a'^\dagger v_b \rangle}_{v_b \left|0\right\rangle_{v_b} = 0} - \mathrm{i} r_a t_b \underbrace{\langle v_a^\dagger b' \rangle}_{\langle 0_{v_a} \left| v_a^\dagger \right. = 0} + r_a r_b \underbrace{\langle v_a^\dagger v_b \rangle}_{=0} \\
&= t_a t_b \langle a'^\dagger b' \rangle \\
&= t_a t_b \left\langle (\aleph u + \mathrm{i} \beth v)^\dagger \, (\mathrm{i} \beth u + \aleph v) \right\rangle \\
&= t_a t_b \left\langle \left(\aleph u^\dagger - \mathrm{i} \beth v^\dagger \right) \left(\mathrm{i} \beth u + \aleph v \right) \right\rangle \\
&= t_a t_b \Big(\mathrm{i} \aleph \beth \langle u^\dagger u \rangle + \aleph^2 \underbrace{\langle u^\dagger v \rangle}_{=0} + \beth^2 \underbrace{\langle v^\dagger u \rangle}_{=0} - \mathrm{i} \aleph \beth \underbrace{\langle v^\dagger v \rangle}_{=0} \Big) \\
&= \mathrm{i} t_a t_b \aleph \beth \langle u^\dagger u \rangle \ . \qquad (3.7)
\end{aligned}
$$

Analogously, one can calculate the remaining expectation values that are of interest, arriving at

$$\langle a^\dagger b \rangle = \mathrm{i} t_a t_b \aleph \beth \langle u^\dagger u \rangle \qquad (3.8)$$

$$\langle ab \rangle = \mathrm{i} t_a t_b \aleph \beth \langle uu \rangle \qquad (3.9)$$

$$\langle a^\dagger a \, b^\dagger b \rangle = t_a^2 t_b^2 \aleph^2 \beth^2 \langle u^\dagger u^\dagger u u \rangle \qquad (3.10)$$

$$\langle a^\dagger a \rangle = \aleph^2 t_a^2 \langle u^\dagger u \rangle \qquad (3.11)$$

$$\langle b^\dagger b \rangle = \beth^2 t_b^2 \langle u^\dagger u \rangle \qquad (3.12)$$

Note for eq. 3.10 that a and $b^\dagger$ do commute, therefore $a^\dagger a b^\dagger b = a^\dagger b^\dagger a b$. Inserting these expressions into the Bell expression $\mathscr{B}(a, b)$ (2.38) gives

$$\mathscr{B} = 2\sqrt{2}\,\frac{\sqrt{\left|\langle a^\dagger b\rangle\right|^2 + |\langle ab\rangle|^2}}{\sqrt{\langle a^\dagger a\, b^\dagger b\rangle} + \sqrt{\langle a^\dagger a\rangle\,\langle b^\dagger b\rangle}} \tag{3.13}$$

$$= 2\sqrt{2}\,\frac{\sqrt{|\mathrm{i}t_a t_b \aleph\beth\,\langle u^\dagger u\rangle\,|^2 + |\mathrm{i}t_a t_b \aleph\beth\,\langle uu\rangle\,|^2}}{\sqrt{t_a^2 t_b^2 \aleph^2\beth^2\,\langle u^\dagger u^\dagger uu\rangle} + \sqrt{\aleph^2\beth^2 t_a^2 t_b^2\,\langle u^\dagger u\rangle^2}} \tag{3.14}$$

$$\mathscr{B}(u) = 2\sqrt{2}\,\frac{\sqrt{|\,\langle u^\dagger u\rangle\,|^2 + |\,\langle uu\rangle\,|^2}}{\sqrt{\langle u^\dagger u^\dagger uu\rangle} + \langle u^\dagger u\rangle}\,. \tag{3.15}$$

We can observe that both loss and reflectivity parameters cancel out due to the unique construction of $\mathscr{B}$. This also holds for losses alone, irrespective of a beamsplitter. Thus, no loss-channel or imbalanced beamsplitter may compromise the entanglement of a source for the Johansen criterion.
Interestingly, this feature depends on the optimal choice in the derivation of $\mathscr{B}(a, b)$. In chapter 2, we chose independent local oscillator amplitudes, like Johansen. THW, on the other hand, decided to set $|\alpha_{\mathrm{LO}}| = |\beta_{\mathrm{LO}}|$. Then, the loss and balance parameters do not cancel because the denominator would then contain $(\langle a^\dagger a\rangle + \langle b^\dagger b\rangle) \diagup 2$ instead of $(\langle a^\dagger a\rangle\,\langle b^\dagger b\rangle)^{1/2}$.
The Johansen criterion quantity $\mathscr{B}'$ analogously translates, by removing the $\langle uu\rangle$ term (either before or after the beamsplitter relations), to

$$\begin{aligned}\mathscr{B}'(u) &= 2\sqrt{2}\,\frac{\langle u^\dagger u\rangle}{\sqrt{\langle u^\dagger u^\dagger uu\rangle} + \langle u^\dagger u\rangle} \\ &= \frac{2\sqrt{2}}{\sqrt{g^{(2)}(u)} + 1}\,,\end{aligned} \tag{3.16}$$

with

$$g^{(2)}(u) = \frac{\langle u^\dagger u^\dagger uu\rangle}{\langle u^\dagger u\rangle^2}\,. \tag{3.17}$$

In fact, the beamsplitter automatically ensures full coherence of first order, i.e.

$$\left|g^{(1)}(u)\right| = \frac{\left|\mathrm{i}t_a t_b \aleph\beth\,\langle u^\dagger u\rangle\right|}{\sqrt{\aleph^2 t_a^2\,\langle u^\dagger u\rangle\,\beth^2 t_b^2\,\langle u^\dagger u\rangle}} = 1\,, \tag{3.18}$$

so only the $g^{(2)}$ part survives. The inequality for $g^{(2)}(u)$, equivalent to $\mathscr{B}'(u) \leq 2$, is then

$$g^{(2)}(u) \overset{\mathrm{LHV}}{\geq} \left(\sqrt{2} - 1\right)^2 \approx 0.172\,, \tag{3.19}$$

so we need only very small $g^{(2)}$ in one mode to meet the entanglement criterion. We will investigate specific states shortly, but before, let us introduce an intuitive reformulation of the criterion for the initial mode.

3.2.1 Photon Statistics Criterion

Alternatively to writing $\mathscr{B}'$ in terms of the second coherence function, one can also express it in the intuitive quantities *mean* μ and *variance* σ^2 of the photon number $N = u^\dagger u$:

$$\mu = \langle u^\dagger u \rangle \tag{3.20}$$

$$\sigma^2 = \left\langle \left(u^\dagger u\right)^2 \right\rangle - \langle u^\dagger u \rangle^2 \tag{3.21}$$

$$= \langle u^\dagger u^\dagger u u \rangle + \mu - \mu^2 \, . \tag{3.22}$$

Rearranging and inserting in (3.16) yields

$$\mathscr{B}' = 2\sqrt{2}\, \frac{\mu}{\sqrt{\sigma^2 - \mu + \mu^2} + \mu} \, . \tag{3.23}$$

The square root in the denominator is always real since $\langle u^\dagger u^\dagger u u \rangle \geq 0$. Therefore $\sigma^2 \geq \mu - \mu^2$. This leads to a region in the μ/σ^2-plane that is generally forbidden. In general, for a non-integer μ, the variance will be larger than zero because then, at least two Fock states (number states) are superposed and thus there is a variance. Only Fock states have vanishing variance σ^2.
These forbidden regions between each pair $(|n\rangle, |n+1\rangle)$ have the form of a parabola of the same shape as the first, $\sigma^2 \geq \mu - \mu^2$, but shifted to the right. The first two can be seen in Fig. 3.2.
The same figure shows the photon statistics in terms of μ and σ^2 and the region that gives violation for the inequality $\mathscr{B}'(u) \overset{\text{LHV}}{\leq} 2$. This region is entirely enclosed in the sub-Poissonian region $\sigma^2 < \mu$, which is inaccessible for classical electrodynamics. The maximal violation with $\mathscr{B}' = 2\sqrt{2}$ is at the arc of the forbidden region, corresponding to states of at most one photon (3.24) The ideal single-photon state is at (1,0) and we see that it is surrounded by a region of $\mathscr{B}'$ violation. Therefore, sufficiently small deviations from the single-photon state will preserve that violation. A coherent state of arbitrary α exhibits Poisson distribution with $\sigma^2 = \mu$.

3.3 Some Interesting Initial States

We will now investigate some states for the beamsplitter input in more detail. Some are in the 'proximity' of the single-photon state and some contrast it. Interestingly, the coherent state appears to be in its proximity, depending on the meaning of this word, *and* shows completely different behaviour.

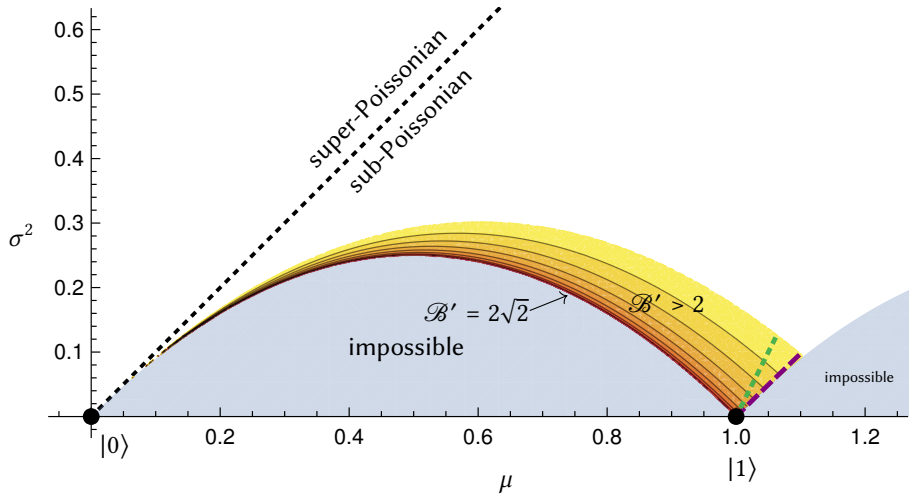

Figure 3.2: The criterion for the beamsplitter input mode in terms of the photon statistics: mean photon number $\mu = \langle n \rangle$ and variance $\mathrm{Var}(n) = \sigma^2 = \langle n^2 \rangle - \langle n \rangle^2$. The orange region depicts $\mathscr{B}' > 2$. $\mathscr{B}'$ is $= 2\sqrt{2}$ (maximal) at the border between the orange and the light blue region, $\mathscr{B}' = 2$ at the border to the white space. Contour lines are shown for $\mathscr{B}' = 2.1, 2.2, \ldots$. The values of $\mathscr{B}'$ below 2 are not plotted. The point $(0, 0)$ corresponds to the zero-photon Fock state $|0\rangle$, $(1, 0)$ to $|1\rangle$, and so forth. The light blue region is impossible even by quantum theory since a superposition of Fock states cannot have vanishing uncertainty in photon number. The superposition $c_0 |0\rangle + c_1 |1\rangle$ maps to the outline of the first blue 'bump'. The region of violation is encompassed by the sub-Poissonian region $\sigma^2 < \mu$. An example for Poissonian light with $\sigma^2 = \mu$ (dotted straight line) is coherent light. The short red and green dashed lines near $|1\rangle$ are the single-photon-added coherent state $u^\dagger |\alpha\rangle$ and displaced coherent state $D_\alpha |1\rangle$, respectively, for values of α with violation.

3.3.1 At Most One Photon

If we consider a general state with only up to one photon, i.e. of the form

$$\rho_{\leq 1\gamma} = \frac{1}{2}\left(p\,|0\rangle\langle 0| + q\,|0\rangle\langle 1| + q^*\,|1\rangle\langle 0| + (1-p)\,|1\rangle\langle 1|\right) , \tag{3.24}$$

we can see that this yields $g^{(2)} = 0$ because $uu\,|1\rangle = uu\,|0\rangle = 0$ and thus maximal violation of the inequality

$$\mathscr{B}' = 2\sqrt{2} \not\leq 2 . \tag{3.25}$$

This holds independent of the parameters p and q. Also incoherent mixtures violate maximally because the coherence is only important *between* the two modes. But this coherence is secured by the beamsplitter.
This is an interesting result, since it means that the source does not need to meet hard requirements on the production rates. Compared to the state $|2\gamma\rangle$ from sec. 2.5, this is more robust since there, only small values of s violate the full inequality, corresponding to a parametric converter with low gain [THW90].
However, let us revisit the statistics criterion and Fig. 3.2. The closer we are to $|0\rangle$, the closer we get to the critical $\mathscr{B}' = 2$ contour. Therefore, we want to be fairly close to the single-photon Fock state $|1\rangle$ if possible. From there, any kind of perturbation in the state can be tolerated, as long as it is sufficiently small: Any perturbation will change μ and σ continuously, so a small change will keep $\mathscr{B}' > 2$.

3.3.2 Not-Exactly-Single-Photon States

We said that not only the single-photon state but also arbitrary deviations from it produce detectable entanglement. Two examples for 'not-exactly-single-photon states' are the *photon-added coherent state* (SPAC) and the *displaced single-photon* state (DSP). Both are connected to the coherent state $|\alpha\rangle$ by the displacement operator [WM94]

$$D_\alpha = \exp\left(\alpha u^\dagger - \alpha^* u\right) , \quad \text{with} \tag{3.26}$$
$$D_\alpha\,|\text{vac}\rangle = |\alpha\rangle_u .$$

This relation is equivalent to the exponential form in (3.30), since $u\,|\text{vac}\rangle = 0$, so only the $u^\dagger$ in D_α survives. Consider the single-photon added coherent state (SPAC state)

$$|\text{SPAC}\rangle = \frac{1}{N_\alpha} u^\dagger\,|\alpha\rangle = u^\dagger D_\alpha\,|\text{vac}\rangle . \tag{3.27}$$

It models a plane-wave background for a single-photon. In the limit of small α, $|\text{SPAC}\rangle$ goes to $|1\rangle$, so we get violation of $\mathscr{B}' \leq 2$ for $\alpha \lesssim 0.225$. For large values of α, the state is similar to the coherent state, and the criterion is not met anymore.

The corresponding statistics of the states is depicted in Fig. 3.2 in the red, dashed line close to the forbidden region.
A similar state is the 'displaced single-photon state'

$$|\mathrm{DSP}\rangle = D_\alpha |1\rangle = D_\alpha u^\dagger |\mathrm{vac}\rangle \ , \tag{3.28}$$

which, for small alpha, is similar again to $|1\rangle$. It is *not* equal to SPAC, since a and $a^\dagger$ do not commute. For $\alpha \lesssim 0.25$, the state also violates the $\mathscr{B}' \leq 2$ inequality. Its statistics is depicted in Fig. 3.2 in the green dashed line.
The SPAC and DSP states show that a classical 'background' radiation in the form of a coherent state may be tolerated. Since $|\alpha|^2$ is the mean photon number for the coherent state, the limit $\alpha \approx 1/4$ implies that the background count rate has to be smaller than $1/16$ of the single-photon count rate.

3.3.3 Coherent State

In contrast to this, consider a coherent state $|\alpha\rangle_u$ at the input of the beam splitter. Coherent states have mean photon mumber $\mu = |\alpha|^2$ and $\sigma^2 = |\alpha|^2$. One can quickly calculate from $u|\alpha\rangle_u = \alpha$ that

$$\begin{aligned} g^{(2)}(u) &= 1 \ , \\ \mathscr{B} &= 2 \leq 2 \ , \\ \mathscr{B}' &= \sqrt{2} \leq 2 \ . \end{aligned} \tag{3.29}$$

In fact, the state behind the beamsplitter is seperable, resulting from the exponential form of the coherent state [WM94]. For a balanced beamsplitter:

$$\begin{aligned} |\alpha\rangle_u &= \mathrm{e}^{-|\alpha|^2/2}\, \mathrm{e}^{\alpha u^\dagger} |\mathrm{vac}\rangle \\ &= \mathrm{e}^{-|\alpha|^2/2}\, \mathrm{e}^{\alpha(a^\dagger + \mathrm{i}b^\dagger)/\sqrt{2}} |\mathrm{vac}\rangle \\ &= \mathrm{e}^{-(|\alpha|/\sqrt{2})^2/2}\, \mathrm{e}^{\alpha a^\dagger/\sqrt{2}}\, \mathrm{e}^{-(|\alpha|/\sqrt{2})^2/2}\, \mathrm{e}^{\mathrm{i}\alpha b^\dagger/\sqrt{2}} |\mathrm{vac}\rangle \\ &= \left| \alpha/\sqrt{2} \right\rangle_a \left| \mathrm{i}\alpha/\sqrt{2} \right\rangle_b \ , \end{aligned} \tag{3.30}$$

which is a separable pure state (see eq. 2.2). This also holds for an arbitrary beamsplitter with $\sqrt{2}$ replaced by reflectivity $\aleph$ and $\beth$, and for arbitrary α. This result is expected since the coherent state is a rather 'classical' state [WM94].
On the other hand, if we choose $|\alpha|$ to be very small, the number of photons per unit time becomes very small, too. This is often associated with 'at most one photon', which might be very intuitive: If only one photon exits the source in every hour, there shouldn't be any multi-photon contributions. The overlap of a coherent state with a Fock state is

$$|\langle n \,|\, \alpha\rangle|^2 = \mathrm{e}^{-|\alpha|^2} \frac{|\alpha|^{2n}}{n!} \ , \tag{3.31}$$

which also suggests that for $|\alpha| \ll 1$, the overlap with $n \geq 2$ can be neglected. However, the result $\mathscr{B} = 2$ holds for any $|\alpha| > 0$. It is therefore crucial *not* to make the approximation

$$|\alpha\rangle \longmapsto \left[\, |0\rangle + \alpha\, |1\rangle \,\right] / N \quad \textit{wrong}, \text{ even for small } \alpha\,. \tag{3.32}$$

We have seen that for any state of the form $c_0\,|0\rangle + c_1\,|1\rangle$, $g^{(2)}(u)$ will vanish. Therefore, neglecting multi-photon events (e.g. for weak coherent states) renders $\mathscr{B}'$ maximal automatically and 'destroys' the classical structure of the coherent state. We will see that taking $|2\rangle$ into account will suffice, because this allows high values of $g^{(2)}$.
While this cosideration was on the basis of input states, a similar conclusion will be presented for in the section on post-selection (3.4), which considers discarding events after the experiment.

3.3.4 At Most Two Photons

Let us look at the inequality from another angle. Consider states of the form

$$|\psi\rangle_{\text{input}} = c_0\,|0\rangle_u + c_1\,|1\rangle_u + c_2\,|2\rangle_u\,, \tag{3.33}$$

i.e. superpositions of the Fock states up to 2 photons. These states cover a range of different phenomena. They contain perfect $\mathscr{B}' = 2\sqrt{2}$ states (for $c_2 = 0$) and also states that violate $\mathscr{B} \leq 2$ but not $\mathscr{B}' \leq 2$, since the $\langle uu\rangle$ part of $\mathscr{B}$ is proportional to $c_0^* c_2$. Furthermore, these states allow us to compare the post-selection schemes in sec. refsecps with the results without this post-selection, since the post-selection can only be calculated for a rather small subset of the whole Hilbert space.
We can restrict to real, positive parameters c_i without loss of generality: The only expectation value in $\mathscr{B}$ where the relative phases play a role is $\langle uu\rangle \propto c_0^* c_2$. But $\mathscr{B}$ is a function of $|\langle uu\rangle|$, so the relative phase drops out. If we included $|3\rangle_u$ at the input state, the relative phase of $c_0^* c_2$ and $c_1^* c_3$ would survive in $\mathscr{B}$. We do not include $|3\rangle_u$ for two reasons: because the $|\langle uu\rangle|$-part is not included in $\mathscr{B}'$, which is of main interest, and because adding $|3\rangle_u$ to the post-selection calculation would be uneconomic.
Figures 3.4 and 3.3 show the values of $\mathscr{B}$ and $\mathscr{B}'$ for the whole parameter set $\{c_0, c_1, c_2\} \geq 0$ as contour plots. Because of normalization, the graph's origin corresponds to $c_0 = 1$, i.e. $|\psi\rangle_{\text{input}} = |0\rangle_u$. The Fock states $|1\rangle_u$ and $|2\rangle_u$ can be found in the lower right and upper left corner, respectively.
The contours of the $\mathscr{B}'$-Plot 3.3 are rather similar to the representation in μ and σ^2: Along the superposition of $|0\rangle$ and $|1\rangle$, $\mathscr{B}'$ is maximal and drops when other contributions are added. Around $|0\rangle$, $\mathscr{B}'$ drops faster than around $|1\rangle$.
Figure 3.4 shows the similar contour plot for $\mathscr{B}$. Compared with $\mathscr{B}'$, this contains an additional region of violation in the lower left. Here, small c_0 and moderately small c_2 give rise to rather large values of $\langle uu\rangle \propto c_0^* c_2$, while the denominator of

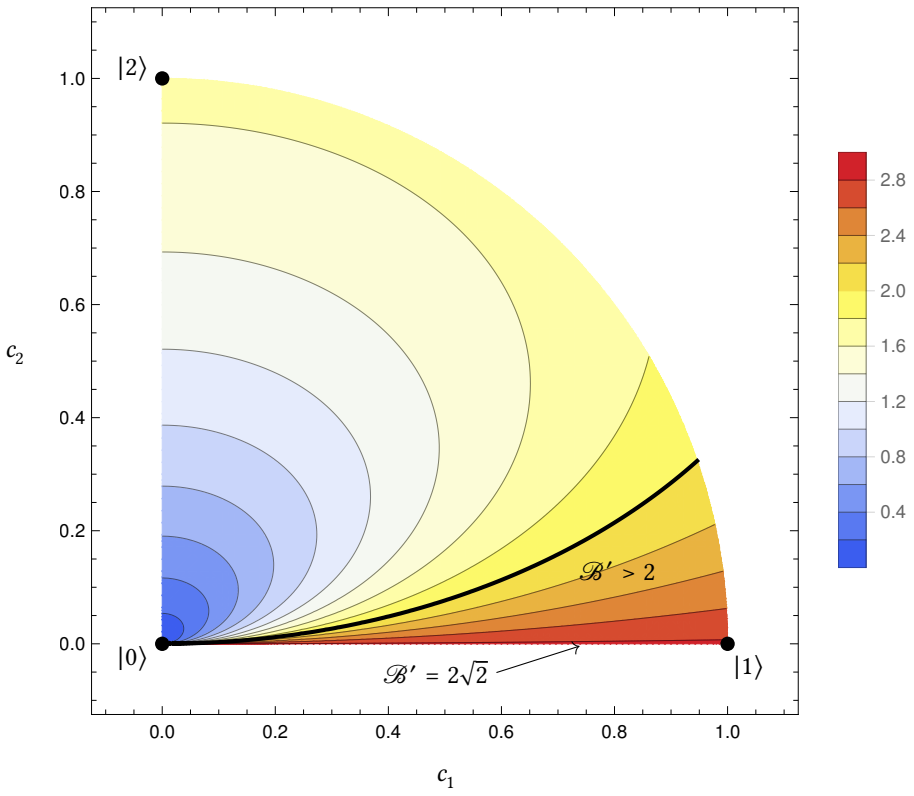

Figure 3.3: Johansen quantity $\mathscr{B}'$ for the Hilbert space of up to two photons. The axes are c_1 and c_2, the amplitudes of $|1\rangle$ and $|2\rangle$. The origin is $|0\rangle$ due to normalization, the lower right corner $|1\rangle$ and the upper left corner $|2\rangle$. $\mathscr{B}'$ is maximally violated for any superposition (or mixture) of $|0\rangle$ and $|1\rangle$, except $|0\rangle$ itself. At $|1\rangle$, the critical ($\mathscr{B}' = 2$)-contour is as far away as possible, it is therefore more robust than e.g. $(|0\rangle + |1\rangle) \diagup \sqrt{2}$.

$\mathscr{B}$ remains rather small, achieving up to the maximal value of $\mathscr{B} = 2\sqrt{2}$.
These findings fit well into our previous results and will allow us to investigate the effect of discarding certain events (post-selection) in sec. 3.4.

3.3.5 Beyond the Johansen Criterion

In order to illustrate that $\mathscr{B}'$ does not cover all entangled states, and not even all states that violate the full $\mathscr{B}$ inequality, we investigate some specific examples. We already saw that in the set of states with at most two photons (sec. 3.3.4), some states violate only $\mathscr{B}$ but not $\mathscr{B}'$. We will revisit $c_0 |0\rangle + c_2 |2\rangle$, introduce the well-known squeezed state and show that the statistics of these states is very different from the single-photon.
States that violate $\mathscr{B}$ but not $\mathscr{B}'$ utilize the $\langle uu \rangle$ term in $\mathscr{B}$. Therefore, we need

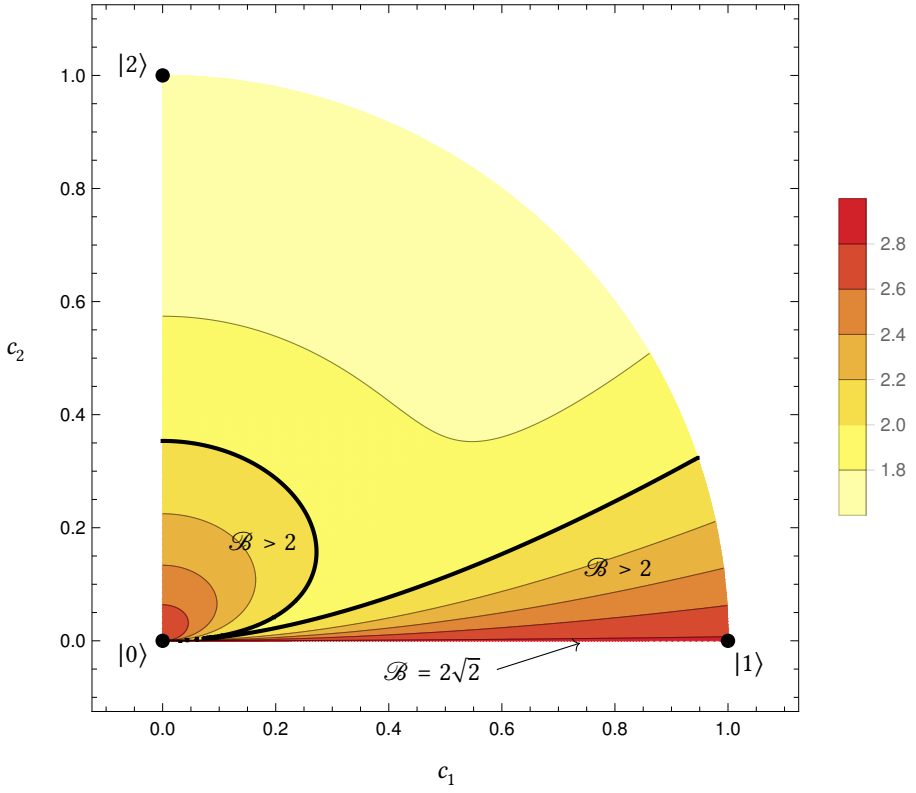

Figure 3.4: Full Bell quantity $\mathscr{B}$ for the Hilbert space of up to two photons. The axes are identical to figure 3.3. $\mathscr{B}$ includes the term $|\langle uu\rangle|$ which is omitted in $\mathscr{B}'$, therefore a second region with $\mathscr{B} > 2$ appears near the origin, at small c_1, large c_0 and moderately small c_2. The overall values are considerably larger due to the additional term $\langle uu\rangle$. The ($\mathscr{B} = 2$)-contour reaches the origin. Weak coherent states ($|\alpha| \lesssim 0.3$) can be approximated with up to two photons. This truncated coherent state lies on the ($\mathscr{B} = 2$)-contour close to $|0\rangle$ (line too short to depict).

states with significant amplitudes for Fock states $|n\rangle$ and $|n+2\rangle$ at the same time, preferably for multiple n. But at the same time, the coincidence $\langle u^\dagger u^\dagger uu\rangle$ and photon rate $\langle u^\dagger u\rangle$ must not become too large.

Squeezed Vacuum

The squeezed vacuum has the peculiar feature that only even-numbered Fock states are populated:

$$|0,\zeta\rangle = c_0\,|0\rangle + c_2\,|2\rangle + \ldots + c_{2n}\,|2n\rangle + \ldots\ . \tag{3.34}$$

It is defined using the unitary (single-mode) Squeezing operator [GK04]

$$S_\zeta = \exp\left[\tfrac{1}{2}\left(\zeta^* uu - \zeta u^\dagger u^\dagger\right)\right] , \tag{3.35}$$

with complex squeezing parameter $\zeta = re^{i\xi}$. It produces a squeezed coherent state if used together with the displacement operator D_α:

$$D_\alpha S_\zeta \left|\text{vac}\right\rangle = \left|\alpha, \zeta\right\rangle \quad \text{squeezed coherent state} \tag{3.36}$$

and squeezed vacuum is the squeezed state swith $\alpha = 0$. The squeezing operator satisfies th following relations with the creation and annihilation operators $u, u^\dagger$ of the form

$$S_\zeta^\dagger\, u\, S_\zeta = u\cosh r - e^{i\xi} u^\dagger \sinh r , \tag{3.37}$$

$$S_\zeta^\dagger u^\dagger S_\zeta = u^\dagger \cosh r - e^{-i\xi} u \sinh r , \tag{3.38}$$

from which the expectation values $\langle uu\rangle , u^\dagger u, \langle u^\dagger u^\dagger uu\rangle$ can be calculated. After a bit of using these identities, we arrive at an expression for $\mathscr{B}$ for the squeezed vacuum state with $\zeta = r$ real:

$$\mathscr{B}_{|0,\zeta\rangle} = 2\sqrt{2}\frac{\sqrt{\left|\cosh r \sinh^2 r\right|^2 + \sinh^4 r}}{\sinh^4 r + \sqrt{\sinh^2 r\left(\cosh^2 r + 2\sinh^2 r\right)}} . \tag{3.39}$$

One finds that $\mathscr{B} > 2$ for $r \lesssim 0.4$. The corresponding statistics is shown in Fig. 3.5 in a red, dashed line. Remarkably, it lies in the super-Poissonian region, similar to the state $c_0 \left|0\right\rangle + c_2 \left|2\right\rangle$.

$c_1 \left|1\right\rangle + c_3 \left|3\right\rangle$

Another interesting state is the superposition of the single-Photon Fock state with the 3–photon Fock state. It covers both $\mathscr{B}'$ by the single-photon part and the $\langle uu\rangle$ part by $c_1^* c_3$. It is also depicted in Fig. 3.5, where it can be seen that the area of $\mathscr{B}$ violation for this state is larger than the region of $\mathscr{B}'$ statistics violation, as expected. While interesting to consider, these states cannot be checked in the simple coincidence–and–interferometer setup.

3.4 Post-selection

We investigated in section 3.3.3 the effect of truncating a coherent state such that only $c_0 \left|0\right\rangle + c_1 \left|1\right\rangle$ survives and showed that this always yields $\mathscr{B}'$ violation because $g^{(2)}(u) = 0$ for these states. This has implications for experiments with low event rates. The two-photon event rate is then naturally even smaller and true 2–photon-events may not be reliably detected. We will therefore investigate how

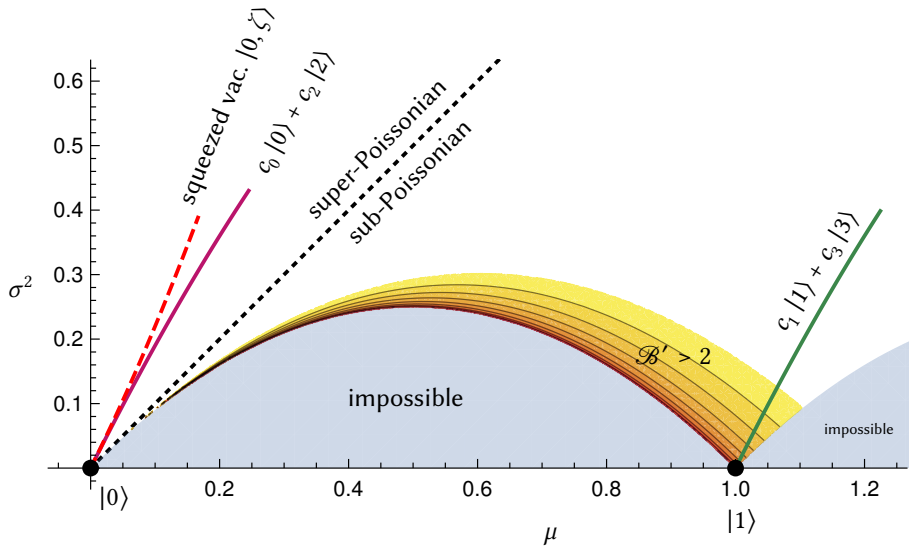

Figure 3.5: Various states that violate the full $\mathscr{B} \leq 2$ inequality for comparison with the photon statistics variant for the $\mathscr{B}'$ criterion. The states are plotted as lines with their respective values of μ and σ^2 for parameters with which they violate $\mathscr{B} \leq 2$. The axis and regions are the same as in figure 3.2. The red dashed line is (μ, σ^2) of the squeezed vacuum state $|\zeta; 0\rangle$ for all ζ such that $\mathscr{B} \leq 2$ is violated. It utilizes the $\langle uu \rangle$-part of $\mathscr{B}$ (3.15) because only even-numbered Fock states are populated. It violates for values of $0 < |\zeta| < 0.4$. For small ζ, it is similar to the two-Fock-state superposition $c_0 |0\rangle + c_2 |2\rangle$ (violet). Both lie, remarkably, in the super-Poissonian region, which is accessible even for classical light. The third state $c_1 |1\rangle + c_3 |3\rangle$ (green) violates both $\mathscr{B}' \leq 2$ for small c_3 and only $\mathscr{B} \leq 2$ for larger c_3 because of $\langle uu \rangle$, up to $c_3 \approx 0.34$.

the measurement of the criterion is affected if we discard events. We call this procedure post-selection. There are other notions of post-selection, e.g. that one discards events where some cross-check measurement yielded an unfavorable result. This is not meant here.
We will only consider post-selecting for states that are produced by a beamsplitter, not general two-mode states, for simplification.
Just before measurement, we apply the projection operator to the wavefunction (or density matrix) and renormalize. For post-selecting events with at least one photon detection, we discard the case that both detectors do not click, i.e.:

$$|\psi\rangle \mapsto \frac{1}{\sqrt{N_\psi}} \left(\mathbb{1} - |0\,0\rangle \langle 0\,0|\right) |\psi\rangle \quad \text{and} \tag{3.40}$$

$$\rho \mapsto \frac{1}{N_\rho} \left(\mathbb{1} - |0\,0\rangle \langle 0\,0|\right) \rho \left(\mathbb{1} - |0\,0\rangle \langle 0\,0|\right) \tag{3.41}$$

Where $|0\,0\rangle$ represents no photons at both detectors in arms A and B. These projection operations have to be performed at the expectation values $\{\langle ab\rangle, ...\}$, in our case at the expression $\mathscr{B}(a, b)$ (2.38) or $\mathscr{B}'(a, b)$ (2.39).
The projection operators cannot be transferred via beamsplitter relations. Therefore, we start with a state at the beamsplitter input, e.g. $|1\rangle_u = u^\dagger |\text{vac}\rangle$ and calculate its propagation through the beamsplitters via the (inverse) beamsplitter relations. We arrive at a 4-mode expression: modes a, b, l_a, l_b where l_a and l_b are the loss modes of the fictious loss-beamsplitters, see Fig. 3.1. We measure only at the modes a and b, so we can disregard and trace-out the loss modes.
The effort to calculate in this 'forward' direction in comparison to the previous 'backwards' direction scales with the complexity of the input state. Every creation operator $u^\dagger$ has to be written as a superposition of output states $a^\dagger, b^\dagger, l_a^\dagger, l_b^\dagger$. After mulitiplying out all these terms, the expressions like $a^\dagger a^\dagger b^\dagger |\text{vac}\rangle$ have to be written as the Fock states $\sqrt{2}\,|2\rangle_a\,|1\rangle_b$. Thus, we restrict ourselves to a class of states with arbitrary superpositions of the Fock states $|0\rangle, |1\rangle, |2\rangle$:

$$|\psi\rangle_{\text{input}} = c_0\,|0\rangle_u + c_1\,|1\rangle_u + c_2\,|2\rangle_u \tag{3.42}$$

$$= \left(c_0 + c_1 u^\dagger + c_2 \frac{1}{\sqrt{2}} u^\dagger u^\dagger\right) |0\rangle_u \tag{3.43}$$

While this state is certainly not general, it covers the part of the Hilbert space of maximal violaton of the $\mathscr{B}'$ inequality for $c_2 = 0$ and allows us to inspect the effect of a perturbing part with c_2. As an extra, we can also formulate a state that violates $B \leq 2$ but not $\mathscr{B}' \leq 2$ because the $\langle ab\rangle$ part of $\mathscr{B}$ grows with $c_0^* \cdot c_2$.
The tedious but straight-forward calculation yields a state ket $|\psi\rangle_{\text{output}}$, depending on $c_0, c_1, c_2, \aleph, t_a$ and t_b. The post-selection projection operators, the renormalizing and the following calculation of expectation values have been automated by a computer algebra program. The output states are then combined into the expressions for $\mathscr{B}$ and $\mathscr{B}'$.
Because of the projection operators, the loss parameters t_a, t_b and the beamsplitter parameter $\aleph$ do not cancel in $\mathscr{B}$ and $\mathscr{B}'$.

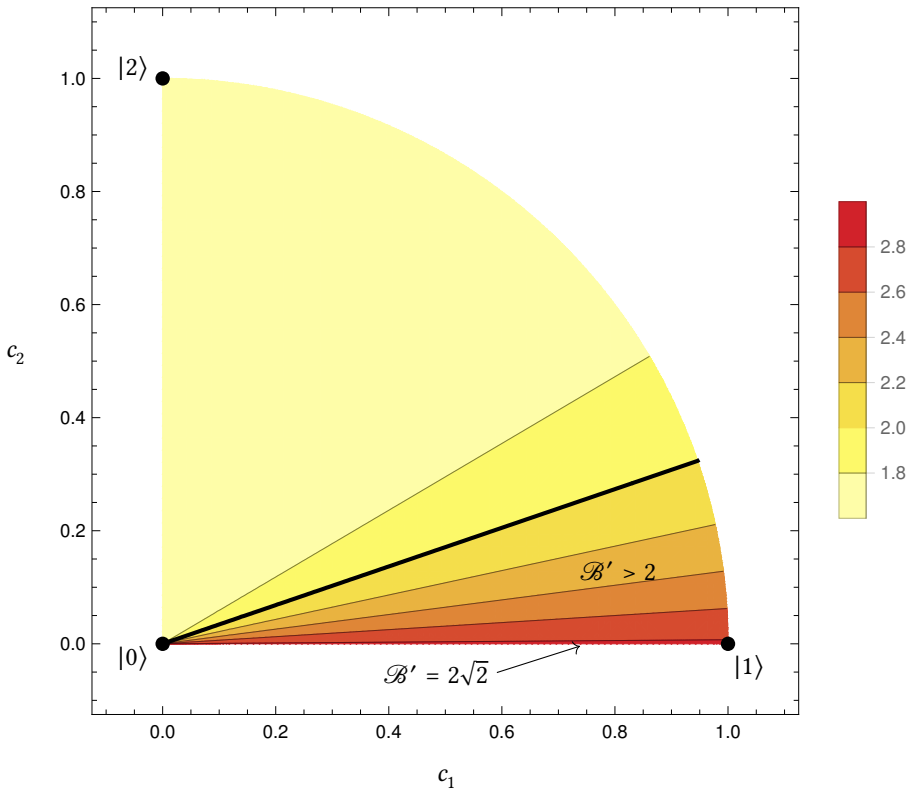

Figure 3.6: $\mathscr{B}'$ for the Hilbert space of up to two photons, like in figure 3.4, with post-selecting events that had at least one detector click, assuming a balanced beamsplitter and no losses. $\mathscr{B}'$ is independent of c_0. At the circle $c_1^2 + c_2^2 = 1$, the value of $\mathscr{B}'$ is equal to the $\mathscr{B}'$ for the case without post-selection. Thus, this plot can be constructed from figure 3.3 by radial projection from the sphere inwards. The area of violation of $\mathscr{B}' \leq 2$ is sufficiently larger than without post-selection (Fig. 3.3).

3.4.1 Post-selecting Events with at Least One Photon

First, we look at the post-selection scheme that discards any events without a photon detection. The projection operator is the one given in eq. 3.40. The resulting $\mathscr{B}$ and $\mathscr{B}'$ depend on $c_0, c_1, c_2, \aleph, t_a$ and t_b. Here, losses and beamsplitter parameters do not cancel out. We can restrict again to real parameters c_i as explained in subsection 3.3.4.

Balanced, Lossless Case

Fig. 3.6 shows $\mathscr{B}'$ for the balanced lossless case, i.e. $t_a = t_b = 0$ and $\aleph^2 = 1/2$. The depicted parameters are the real coefficients c_1 and c_2. The plot therefore covers all the pure Fock states as input: $|0\rangle$ for $c_1 = c_2 = 0$, $|1\rangle$ for $c_1 = 1$ and $|2\rangle$

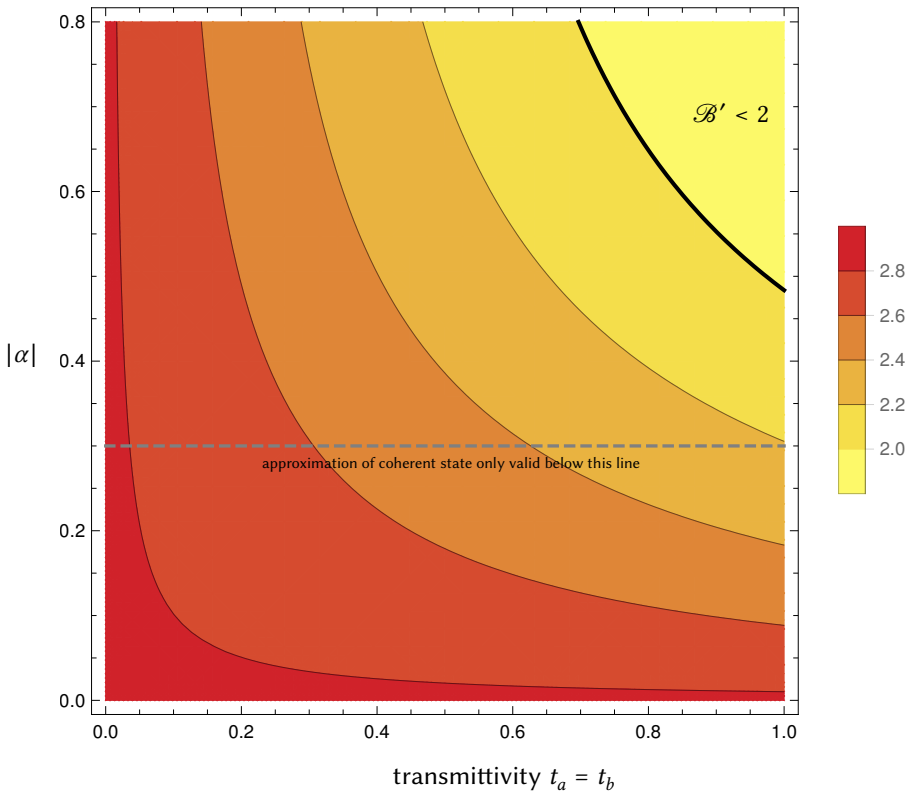

Figure 3.7: $\mathscr{B}'$ for a coherent input $|\alpha\rangle_u$, imbalanced beamsplitter, balanced losses and post-selecting events with at least one detector click. The lower axis is the transmittivity amplitude $t_a = t_b = \sqrt{1 - \text{loss}}$) of each arm, i.e. the most loss is to the left; the left axis is the modulus of the coherent state parameter $|\alpha|$. Even though the coherent state is a classical input, post-selecting at-least-one-photon events renders the outcome to 'entangled'. Furthermore, loss increases $\mathscr{B}'$. Note that this plot is a result of approximating the coherent state with a state of at most two photons. As explained in the text, this approximation is only valid for $|\alpha| \lesssim 0.3$. The upper part is included to show that $\mathscr{B}' \leq 2$ is possible in this approximation.

for $c_2 = 1$, i.e. at the corners. The Contours are radial, i.e. the c_0 part does not matter at all. Instead, the ratio of c_1 and c_2 determines the value of $\mathscr{B}'$. Without the post-selection (Fig. 3.3), this is not the case. Here, the Fock state $|1\rangle$ is more robust than the superposition $c_0 |0\rangle + c_1 |1\rangle$.

Coherent state

Since the post-selection scheme ensures violation of the $\mathscr{B}' \overset{\text{LHV}}{\leq} 2$ inequality even for states with rather small $\mathscr{B}'$ without post-selection, we can even get classical

radiation to violate the inequality, using our scheme. Consider the single-mode coherent state $|\alpha\rangle_u$, defined via $u\,|\alpha\rangle_u = \alpha\,|\alpha\rangle_u$ at the input. As discussed in section 3.2, this state yields $\mathscr{B}' = \sqrt{2} \leq 2$ without post-selection. The Fock-state representation for the coherent state is

$$|\alpha\rangle_u = \mathrm{e}^{-\frac{|\alpha|^2}{2}}\,\mathrm{e}^{\alpha u^\dagger}\,|\mathrm{vac}\rangle \tag{3.44}$$

$$= \mathrm{e}^{-\frac{|\alpha|^2}{2}} \sum_{n=0}^{\infty} \frac{\alpha^n}{\sqrt{n!}}\,|n\rangle\,, \tag{3.45}$$

so for small $|\alpha|$, only Fock states $|n\rangle$ with small n are macroscopically populated. We showed that neglecting $n \geq 2$-Fock states makes $g^{(2)}(u) = 0$ and thus $\mathscr{B}' = 2\sqrt{2}$ automatically. However, keeping the $|2\rangle$ term suffices to allow for finite $g^{(2)}(u)$. Thus, for $|\alpha| \leq 0.3$, a coherent state can be approximated to fairly good accuracy with only three Fock states $\{|0\rangle, |1\rangle, |2\rangle\}$, since $|\langle n = 3\rangle\,\alpha = 0.3|^2 \approx 10^{-4}$. Then,

$$|\alpha\rangle_u \approx \frac{1}{\sqrt{N}}\left(|0\rangle_u + \alpha\,|1\rangle_u + \frac{\alpha^2}{\sqrt{2}}\,|2\rangle_u\right) \quad \text{with } N = 1 + \alpha^2 + \frac{\alpha^4}{2}. \tag{3.46}$$

This state shows $\mathscr{B}' \approx \sqrt{2}$ for $|\alpha| \leq 0.3$, just like the full coherent state.
If we now introduce post-selection on this state, we can investigate its effect on the coherent state. Figure 3.7 shows $\mathscr{B}'$ for this truncated coherent state, using post-selection, with some other parameters fixed and one loss parameter t_a variable. We find that discarding the no-click events indeed yields values for $\mathscr{B}'$ larger than 2, which is impossible without postselection. In fact, it seems to be impossible to find values for the parameters $\aleph, t_a$ and t_b for which $\mathscr{B}' \leq 2$ for $\alpha \leq 0.3$. Additionally to the importance of the two-photon events, we see that also events, or experimental runs, without photon clicks have to be taken into account in order to not overestimate $\mathscr{B}'$ and get a 'false positive' for entanglement detection.

3.4.2 Post-selecting Events with at Most One Photon

We have seen in the section 3.2 that input states with at most one photon exhibit maximal violation of the Bell inequality. Thus, it is intuitive that post-selecting events whith *at most* one detector click should provide a likely violation as well. We use the projection operator given by

$$|\psi\rangle \mapsto \frac{1}{\sqrt{N_\psi}}\left(\mathbb{1} - |1\,1\rangle\langle 1\,1| - |2\,0\rangle\langle 2\,0| - |0\,2\rangle\langle 0\,2|\right)\,|\psi\rangle \tag{3.47}$$

to discard any events with two detector clicks. The projection operator calculation yields $\mathscr{B} = \mathscr{B}' \equiv 2\sqrt{2}$, independent from parameter choice. We can understand this if we consider $g^{(1)}$ and $g^{(2)}$ (as defined in eq.s 2.41 and 2.42). $g^{(2)}$ has to vanish: Any state that is produced after beamsplitter and loss will have its $|1\,1\rangle$ part removed. Therefore, there are no coincidences and $g^{(2)} = 0$. The first-order coherence was shown to be fulfilled for beamsplitter-ouptputs of arbitrary parameters

in sec. 3.2. Any state that results from the post-selection could also arise from an input without postselection, thus $|g^{(1)}(u)| = 1$ still holds.
The case of **exactly on photon** is contained in 'at most one photon' and thus yields $\mathscr{B} \equiv 2\sqrt{2}$ for all inputs.
The post-selection calculations have confirmed that it makes a big difference if we include all possible outcomes or discard events, especially two-photon events. Discarding two-photon events makes it impossible to obtain any other value for $g^{(2)}$ than zero.
We did not look at general two-mode states in this post-selection calculation but only at beamsplitter-outputs. This is justified because the first order-coherence $g^{(1)}$ can be unity both for single-photon states and for rather classical coherent states (see sec. 2.5). Post-selecting a coherent state, such that only the single-photon state remains, would not change $g^{(1)}$ but only $g^{(2)}$.

3.5 Discussion of a Different Proposal

Lee and Kim [LK00] have proposed a different way of demonstrating nonlocality of a single photon. Due to its experimental simplicity, it has gained some attention in the field of x-ray quantum optics. References [PKE09] [LP14] and [Lau14] have proposed to use it to verify an entanglement generation by nuclear forward scattering. It was also investigated for implementation with Mössbauer nuclei in thin-fim cavities [Zha16].
Lee and Kim derived a Bell inequality which can be tested using only a Mach-Zehnder interferometer with independent phase shifts. We present the proposal and show in the following why we focused on the work of Johansen Johansen [Joh96] instead.
The setup according to Lee and Kim is the same as in figure 2.4, with a balanced beamsplitter instead of a general source.
A single photon enters the interferometer at the first beamsplitter while its other port remains empty. Alice and Bob are located spatially separate at the two interferometer arms, where they can introduce local phase shifts ϕ_a and ϕ_b by inserting wave plates. Without wave plates, the total relative phase is such that all photons exit the second, balanced, beamsplitter at port C and none at port D.
Lee and Kim consider four measurement settings of the local phases:

Setting	Alice's phase	Bob's phase
$\emptyset$	0	0
A	ϕ_a	0
B	0	ϕ_b
AB	ϕ_a	ϕ_b

The locality argument considers what type of local actions of Alice or Bob may affect the photons to go to D instead of C.

"[...] we assume that those photons that do not change their paths and still arrive at D_C, both when Alice, not Bob, uses her phase shifter, and when Bob, not Alice, uses his phase shifter, will still not change their paths and still arrive at D_C when both Alice and Bob use their phase shifters."
They do not give a more general formulation of locality but call this statement a single-particle version of the locality assumption.
Let the set of photons that arrive at D for setting i be S_i, with $i \in \{A, B, AB\}$. "The photons that do not change their paths" are therefore the complementary sets $S \setminus S_i$, where S is the set of all photons. In set theoretic language, Lee and Kim's locality assumption then reads

$$\left(S \setminus S_A\right) \cap \left(S \setminus S_B\right) \subseteq \left(S \setminus S_{AB}\right) . \tag{3.48}$$

This implies for the cardinality $|\cdot|$, or number of elements,

$$\left|\left(S \setminus S_A\right) \cap \left(S \setminus S_B\right)\right| \leq \left|\left(S \setminus S_{AB}\right)\right| . \tag{3.49}$$

Let the total photon number be $N = |S|$ and the photon number of the other sets be $|S_i| = N_i$. Then, it follows for the left-hand side that

$$N - N_A - N_B \leq |(S \setminus S_A) \cap (S \setminus S_B)| . \tag{3.50}$$

The cardinality of the right-hand side of (3.48) is $N - N_{AB}$ and therefore

$$\begin{aligned} N - N_A - N_B &\leq N - N_{AB} \\ N_{AB} - N_A - N_B &\leq 0 . \end{aligned} \tag{3.51}$$

For convenience, let us formulate this in relative count rates and define the quantity

$$\mathscr{L} := \frac{1}{N}\left(N_{AB} - N_A - N_B\right) \leq 0. \tag{3.52}$$

This inequality on the count rate at detector D is violated by quantum theory: The count rate can be calculated with the tools presented in section3.2. For arbitrary phases φ_a, φ_b at Alice and Bob, one finds

$$\langle d^\dagger d \rangle = \sin^2\left(\frac{\varphi_a - \varphi_b}{2}\right) N . \tag{3.53}$$

Replacing the phases for N_A, N_B, and N_{AB} accordingly, one arrives from (3.52) at

$$\mathscr{L}_{QT} = \sin^2\left(\frac{\phi_a - \phi_b}{2}\right) - \sin^2\left(\frac{\phi_a}{2}\right) - \sin^2\left(\frac{\phi_b}{2}\right) \overset{?}{\leq} 0 . \tag{3.54}$$

This inequality is violated for e.g. $\phi_a = -\phi_b = \phi$ and a small-angle-approximation $\sin x \approx x$, yielding $\phi \geq \sqrt{2}\phi$.
Maximal violation is achieved with $\phi_a = -\phi_b = \pi / 3$ with

$$\mathscr{L}_{QT} = \tfrac{1}{4} \geq 0 . \tag{3.55}$$

Criticism

The following criticism of Lee and Kim's proposal is twofold. Firstly, we argue that the inequality's prerequisites constrain the inequality's applicability to a very small set of states, so that it cannot serve as an entanglement criterion. Secondly, we argue that the presented locality principle is not convincing.

The prerequisites

The first prerequisite is to start with a single photon as the input for the experiment. Other imput states are not allowed. Usually, a Bell inequality is defined using measurements that can be obtained regardless of the present state. For some state, the measurements will yield violation (thus follows that these states were entangled) and for others, the measurements yield no violation, which is compatible with local hidden variables.
Any sensible notion of a single photon, not only in quantum theory, would predict that this single photon can only be detected once in a photon-counter. Thus, the coincidence measurement, as depicted in figure 2.5, would yield no coincidences and therefore, in QT language, $g^{(2)} = 0$.
The second prerequisite is that no photons exit the output port D of the second beamsplitter in setting "$\varnothing$", i.e. if neither Alice nor Bob uses their phase shifter. Let us consider the interference visibility at detector D (see sec. 2.4.3): It quantifies the contrast of maxima and minima of an interference pattern in the range $[0, 1]$ [WM94, p. 34]:

$$\mathrm{VIS} = \frac{I_{\max} - I_{\min}}{I_{\max} + I_{\min}}. \tag{3.56}$$

Since detector D detects no photons in the setting "$\varnothing$", $I_{\min} = 0$ and thus VIS = 1. The visibility can be related to the first-order coherence function $g^{(1)}$, as demonstrated in sec. 2.4.3:

$$\mathrm{VIS} = |g^{(1)}| \, \frac{2\sqrt{I_\mathrm{A} I_\mathrm{A}}}{I_\mathrm{A} + I_\mathrm{B}} \,, \tag{3.57}$$

where $I_{\mathrm{A/B}}$ are the intensities of the two beams inside the interferometer and $g^{(1)}$ is defined as in (2.41). It follows that

$$\mathrm{VIS} \leq |g^{(1)}| \,, \tag{3.58}$$

such that the full visibility VIS = 1 implies $|g^{(1)}| = 1$.
The prerequisites thus restrict the criterion's applicability to the ideal case of a single photon with full coherence, i.e. the single-photon entangled state $|\mathrm{SPE}\rangle$ (2.53) Applying the criterion to different states is not allowed because these cannot satisfy the prerequisites. If one wants to detect entanglement, this proposal

is therefore unsuitable.
One might argue that the prerequisites may be relaxed. Let us relax the requirement of a single photon in a natural way: If the input is only required to have one photon on average, i.e. $\langle N \rangle = 1$, rather than exactly one single photon, $g^{(2)}$ would not need to vanish. But the coherent state $|\alpha\rangle$ with $\langle N \rangle = |\alpha|^2 = 1$ would then also be admissable. It yields the same results for the count rates (3.53) as the single photon and therefore violates inequality (3.54). The state after the first beamsplitter is, however, separable (2.2), i.e. of the form $|\psi\rangle_a \, |\phi\rangle_b$, and therefore not entangled:

$$\begin{aligned} |\alpha\rangle_u &= \mathrm{e}^{-|\alpha|^2/2} \, \mathrm{e}^{\alpha u^\dagger} \, |\mathrm{vac}\rangle \\ &= \mathrm{e}^{-|\alpha|^2/2} \, \mathrm{e}^{\alpha(a^\dagger + \mathrm{i}b^\dagger)/\sqrt{2}} \, |\mathrm{vac}\rangle \\ &= \mathrm{e}^{-(|\alpha|/\sqrt{2})^2/2} \, \mathrm{e}^{\alpha a^\dagger/\sqrt{2}} \, \mathrm{e}^{-(|\alpha|/\sqrt{2})^2/2} \, \mathrm{e}^{\mathrm{i}\alpha b^\dagger/\sqrt{2}} \, |\mathrm{vac}\rangle \\ &= \left| \alpha \,/\, \sqrt{2} \right\rangle_a \left| \mathrm{i}\alpha \,/\, \sqrt{2} \right\rangle_b , \end{aligned} \tag{3.59}$$

As Lee and Kim's inequality would therefore be violated by a separable state, we may not relax the requirement of a single-photon input in that natural way. It seems difficult to find a sensible relaxation that does not include the coherent state and still lifts the restriction to the ideal single-photon case.
The second prerequisite, that all photons go to C when neither Alice nor Bob use their phase shifter, may not be relaxed. The reasoning of 'photons that change their paths' is based on this prerequisite since any photon that arrives at D only does so because of Alice's or Bob's actions.

Locality Assumption

Finally, their locality assumption is questionable. It is neither derived from a more general locality principle, nor is it convincing on its own. Since any operation of Alice or Bob has a natural, causal effect on the physical state after the recombination, locality should not restrict the measurements at the detectors behind the beamsplitter.
Asher Peres defines locality in ref. [Per02], [p. 160]: "[the principle of local causes ...] asserts that events occurring in a given spacetime region are independent of external parameters that may be controlled, at the same moment, by agents located in distant spacetime regions." In a usual Bell test, like the one described in section 2.2, the events are the measurements of two separated physical subsystems without the possibility of communication. In Lee and Kim's proposal, the distant events are the actions of Alice and Bob that alter two separated physical sub-systems that are combined later. Only on this combined system, measurements are performed. This is not merely a 'loophole', which is common in imperfect Bell experiments, but necessary: without recombining the beams, the interference cannot be measured, and the inequality cannot be obtained.

To summarize, the presented inequality cannot act as an entanglement criterion due to the strict prerequisites. Additionally, its validity is questionable due to the specific locality assumption that is used.

Chapter 4

Applications in Hard X-Ray Regime

This chapter summarizes the previously obtained requirements to generate and detect states that violate the Bell inequality introduced in chapter 2. Recent proposals and experimental techniques in the hard x-ray regime are then discussed in view of these requirements. We investigate Mössbauer nuclei in thin-film cavities in more detail, deriving a scheme to extract the coherence of first order from its Fano spectrum.

4.1 Summary of Requirements

When searching for realizations of entanglement generation and detection in the hard x-ray regime, the following requirements can be inferred from the considerations in chapters 2 and 3:

Requirements for the Source

For a two-mode source, the equal-time coherences of first (2.41) and second order (2.42) have to be measured in an interferometer and a coincidence setup. If the following inequality holds true:

$$\mathscr{B}' = 2\sqrt{2}\,\frac{|g^{(1)}|}{1+\sqrt{g^{(2)}}} > 2\,, \tag{4.1}$$

then an entangled state is present. The measurements of $g^{(1)}$ and $g^{(2)}$ may be performed with losses in the two modes without impairing the validity. The violation implies that the proper Bell experiment would refute local hidden variable theories for the same state. The necessary, but nor sufficient requirements on $g^{(1)}$

and $g^{(2)}$ are

$$|g^{(1)}| > \frac{1}{\sqrt{2}} \approx 0.707 \,, \quad \text{and} \tag{4.2}$$

$$g^{(2)} < \left(\sqrt{2} - 1\right)^2 \approx 0.172 \,. \tag{4.3}$$

If either one of these are not satisfied, the criterion cannot be fulfilled and no entanglement can be detected by this method.

Single-Mode Source + Beamsplitter

If using a beamsplitter to generate two spatial modes from a single mode u, the coherence of first order is equal to unity in theory (sec. 3.2), leaving only the second order coherence $g^{(2)}(u)$ (3.17). The remaining requirement for the single input mode is

$$\mathscr{B}' = 2\sqrt{2}\frac{1}{1 + \sqrt{g^{(2)}(u)}} > 2 \,, \quad \text{or equivalently}$$

$$g^{(2)}(u) < \left(\sqrt{2} - 1\right)^2 \approx 0.172 \,.$$

Then, the input produces an entangled state detectable by the Johansen criterion after impinging on the beamsplitter.
The beamsplitter has to achieve a reasonable spatial separation of the output beams, but may induce significant losses and does not need to be balanced.

Requirements for Detection Instruments

The interferometer for the measurement of $|g^{(1)}|$ has to be capable of sufficiently high interference visibility. For a usual interferometer, such as a Mach-Zehnder interferometer, VIS $\leq |g^{(1)}|$ (see sec. 2.4.3), therefore the minimum requirement for the interferometer is

$$\text{VIS} > 1 \nearrow \sqrt{2} \approx 0.707 \,. \tag{4.4}$$

The higher the interferometer's visibility, the more sensitive is the detection apparatus. In particular, if the source emits modes of unequal intensity, the interferometer has to compensate this with appropriate beamsplitter coefficients in order to produce a sufficiently high interference visibility.

A coincidence counting experiment does not require high detector efficiencies due to the criterions tolerance toward loss. But usually the count rates for such an experiment are low, thus the background rate has to be very small in order to measure $g^{(2)} \ll 1$.
When using a beamsplitter source, it is useful to test the $g^{(1)}$-part, even though it has been theoretically shown that $|g^{(1)}| = 1$ in this case: To derive this result, we used the standard quantum theory description of a beamsplitter. However, an experimental beamsplitter could in principle behave differently. An extreme example: if the beamsplitter produced classical mixtures of incoming single photons, $g^{(1)}$ would vanish and render interferometry impossible.

4.2 Possible Experimental Realizations

In the context of this work, proposals for hard x-ray entanglement fall in 4 categories: two-mode sources of entanglement, beamsplitters, single-photon sources, and interferometers. The available instrumentation for beamsplitters and interferometers is quite adequate to our requirements.

Two-Mode Sources

X-Ray Parametric Down-Conversion

Parametric down-conversion (PDC) is the process of one *pump* photon into two photons (*signal* and *idler*) inside a crystal. It is the most important source for polarization entangled photon pairs in the optical regime. In the hard x-ray regime, PDC has also been realized; a nice overview can be found in [Ada03]. Recent progress has been made in the generation of polarization-entangled photon pairs [SH11]. As [THW90] have shown, the ouput of a parametric down-converter with low conversion gain violates the full Bell inequality $\mathscr{B} \leq 2$, which corresponds to the $\langle ab \rangle$-part of $\mathscr{B}$. It does not, however, violate $\mathscr{B}' \leq 2$ as discussed in 2.5, which is required for our scheme. PDC is also a source for 'heralded' single photons: Triggered by the presence of the idler photon, the actual experiment is performed with the signal photon (see below).

Nuclear Forward Scattering

Pálffy, Keitel, and Evers [PKE09] have proposed to generate entangled single-photon states by coherently controlling a nuclear forward scattering sample via magnetic field rotations [Shv+96]. Liao and Pálffy [LP14] propose a similar scheme for entanglement generation of counter-propagating modes, [Lau14] is a variation thereof. The decay width of the ^{57}Fe nuclei is of the order of nanoelectronvolts; which is very narrow compared to the synchrotron's spectral intensity. Thus, at most one resonant photon per pulse is present and a single, collective excitation describes the state to a very good approximation. The schemes utilize two different decay channels, either at different times [PKE09] or in different directions [LP14] [Lau14]. A single-photon entangled state is said to be generated. The proposals treat the synchrotron pulse as a classical electromagnetic field and the resonant nuclei as a multi-level system. The calculated scattered radiation is a classical field as well.
In chapter 3, it was shown that a beamsplitter with a coherent input cannot produce an entangled state. This raises the question whether this is different for nuclear excitations and a classical pulse. While more than one excitation is infrequent in NFS experiments with synchrotrons, higher excitation numbers are not ruled out. Definite answers to this may not be derived from the results of this thesis, and further calculations using a quantized treatment of the radiation would certainly be of interest for these systems.

Beamsplitters

There are several beamsplitter types available for hard x-rays, covering a wide energy range. Recently, [Osa+13] have reported the fabrication of a silicon Bragg beamsplitter for hard x-rays up to 18.88 keV that preserves the synchrotron or XFEL wavefront. Tuning the incidence angle and thickness to the wavelength of the impinging beam, its reflectivity is on the order of 50 % with 40 % transmittivity, with losses below 10%. The reflected and transmitted (refracted) beams are spatially well separated. [Kun+97] have reported the measurement of $g^{(2)}$ of monochromatized 14.4 keV synchrotron radiation pulses with a silicon beamsplitter in (2 2 0) Laue geometry. This energy range is interesting for applications in nuclear quantum optics since it is the transition energy for the prototype Mössbauer isotope ^{57}Fe [HT99].

Single-Mode Sources

Usual sources of x-rays do no exhibit low values of $g^{(2)}(u)$. While weakening a signal leads to low coincidence rates, its overall count rate is decreased as well, leaving the normalized quantity $g^{(2)}(u)$ (eq. 3.17) unchanged. A synchrotron produces light with $g^{(2)}(u) \gtrsim 1$, corresponding to Poissonian or slightly super-Poissonian statistics, as can be seen e.g. in Ref. [Kun+97]. In nuclear quantum optics experiments at synchrotron light sources, on average less than one resonant photon per pulse is present due to the narrow nuclear line widths. Therefore, the resulting effects are often called 'single-photon effects'. This is, however, different from our sense of a single photon, which would require $g^{(2)}(u)$ to vanish. Radioactive decay is a similar case: With a low angular acceptance of the isotropic emission and / or a reasonably small probe activity, very few clicks per unit time may persuade to calling the process 'single photon'. But radioactive decay exhibits Poissonian statistics, therefore $g^{(2)}(u) = 1$.

X-Ray Parametric Down-Conversion

As discussed, PDC produces photon pairs $|1\rangle_{\text{signal}} |1\rangle_{\text{idler}}$. This can be used to construct a 'heralded' single-photon source, triggering on the idler photon to perform the experiment with the signal photon. Liao, Keitel, and Pálffy [LKP16] proposed such a heralded single photon for the x-ray regime. Since the idler photon is only used as a herald, it doesn't need to be an x-ray photon. Consequently, [LKP16] suggested an the PDC of an x-ray photon into one x-ray photon and one extreme ultraviolet photon, as reported in [TI07] and [Tam+11]. Since the energy of the idler photon is not critical, a higher conversion rate compared to x-ray → x-ray + x-ray may be achieved by exploiting more degrees of freedom.
An interesting proposal to circumvent the problem of low count rates is the 'parasitic mode' [Ada03]: An xPDC crystal is installed permanently in a synchrotron beamline. Due to the low conversion rate, almost all of the incoming photons

propagate through the crystal and can be used for other experiments. The down-converted photons, which change their transverse momentum, can be used in parallel.

Interferometers

The challange for interferometers in the hard x-ray regime is positioning and stabilizing multiple mirrors and beamsplitters with an accuracy of a few ångström.

Single-Crystal Interferometer

This has been overcome for example by cutting all the optical components from a single crystal, leaving them connected by a base and thus keeping them aligned. Using a perfect silicon single-crystal, Bonse and Hart have built such a 'monolithic' interferometer using the (2 2 0) Laue reflection for both the beamsplitter, the analyzer beamsplitter and the two mirrors [BH65]. This is now known as the Triple-Laue (LLL) configuration [BG77]. Since every component is based on crystal diffraction in the same crystal plane, the 'mirrors' are also beamsplitters and direct half of the intensity away from the analyzer beamsplitter. The other half is recombined on the analyzer beamsplitter. The first report of a LLL interferometer [BH65] already achieved an interference visibility of ≈ 91 %, using copper Kα radiation and an acrylic glass wedge of micrometer thickness as a variable phase shifter.
This kind of interferometer could provide an apt way of measuring both $g^{(1)}$ and $g^{(2)}$ at the same time: half the photons enter the interferometer and thus form an interference pattern, which can be used to measure $|g^{(1)}|$. The other half exits the system at the 'mirrors' and can thus be used to measure the coincidence and thus $g^{(2)}$. As discussed in chp. 3, these significant losses in the individual experiments have no effect on $|g^{(1)}|$ and $g^{(2)}$. Interferometer technology has since evolved and stable multi-crystal interferometers with large spatial separation are available. Tamasaku, Yabashi, and Ishikawa [TYI02] report a interferometer with ~ 50 cm separation of the beams for 18.8 keV photons.
A different type of interferometer is investigated in more detail in the next section.

4.3 Interference Visibility in Thin-Film Cavities

In [Hee+15b], Heeg et al. reported the observation of and explained Fano spectra in the reflectance of thin-film cavities containing a layer of Mössbauer ^{57}Fe nuclei. The cavity is irradiated by monochromatized 14.4 keV synchrotron pulses under a grazing incidence angle, close to a deep reflectance minimum of the cavity for light off-resonant to the nuclei. The Fano line shapes arise from the interference of two quantum paths: The empty cavity path $r_{\mathrm{cav}} \mathrm{e}^{\mathrm{i}\phi_{\mathrm{cav}}}$, and the path with interaction with the nuclei, $r_{\mathrm{nuc}}\, \mathrm{e}^{\mathrm{i}\phi_{\mathrm{nuc}}}$. Both channels contain multiple reflections in the cavity. Thus, the system acts as an interferometer with two arms, raising the

question whether it could be used to test the $g^{(1)}$ part of the Johansen criterion. Provided it is capable of a high interferometer visibility, implying high coherence, a single-photon input would generate an entangled state inside the cavity, entangling the mode that interacts with the nuclei and the mode of the empty cavity.
Let us assume that the cavity is constructed such that a deep reflective minimum is achievable for some incidence angle δ_{min} and that the collective effects speed up the decay to high superradiance [Rö+10]. Then, the reflectance of the cavity can be written as [Hee14]

$$\left|R_q(\epsilon)\right|^2 = a_0 \left| r_{\text{cav}}\, \mathrm{e}^{\mathrm{i}\phi_{\text{cav}}} + r_{\text{nuc}}\, \mathrm{e}^{\mathrm{i}\phi_{\text{nuc}}} \right|^2 \tag{4.5}$$

$$= \left| \frac{1}{q - \mathrm{i}} + \frac{1}{\epsilon + \mathrm{i}} \right|^2 . \tag{4.6}$$

Here, $q \propto \Delta\theta^{-1}$ is the Fano parameter, experimentally controlled by the incidence angle $\Delta\theta$. The dimensionless energy detuning ϵ is shifted by $\Delta\theta$ but this shift is constant at constant q. The constant porportionality factor a_0 depends on cavity structure and will be taken to be unity for simplicity.
Due to the phases ϕ_{cav} and ϕ_{nuc}, the system exhibits interference phenomena, resulting in Fano line shapes. The Fano reflectance for $q = 1$ is plotted in Fig. 4.1 in the blue, solid line. Destructive interference occurs at $\epsilon = -q$, corresponding to a relative phase of $\Delta\phi = \pi$ (red dashed line in the plot) and thus a relative minus sign for the amplitudes r_{nuc} and r_{cav}. However, the Fano maximum is not at constructive interference with vanishing relative phase but arises from a combination of interference and decaying amplitude $r_{\text{nuc}} \sim 1 \,/\, \epsilon^2$. The relative phase does not change constantly like in a Mach-Zehnder interferometer and total constructive interference is not possible for any choice of q.
Thus, we can not directly obtain the coherence $|g^{(1)}|$ from the interference visibility as in section 2.4.3. We will now present a scheme to extract the coherence in a different manner.

Extracting the Coherence

To obtain a quantity similar to the standard visibility (sec. 2.4.3)

$$\text{VIS} \frac{I_{\text{max}} - I_{\text{min}}}{I_{\text{max}} + I_{\text{min}}} , \tag{4.7}$$

we will choose certain values of q and ϵ to evaluate I_{min} and I_{max}. Let us choose $q = 1$ and consider the two points $\epsilon = -1$ and $\epsilon = +1$ in the resulting Fano spectrum, plotted in Fig. 4.1. The cavity amplitude r_{cav} is equal for both points due to constant q. The nuclear amplitude r_{nuc} is equal for both points because of the dependence on ϵ^2. Thus, we can define a visibility that is only dependent on varying phases, i.e. *interference*, and not varying amplitudes. We are in the minimum at $\epsilon = -1 = -q$, which benefits the visibility. Because of the choice $q = 1$,

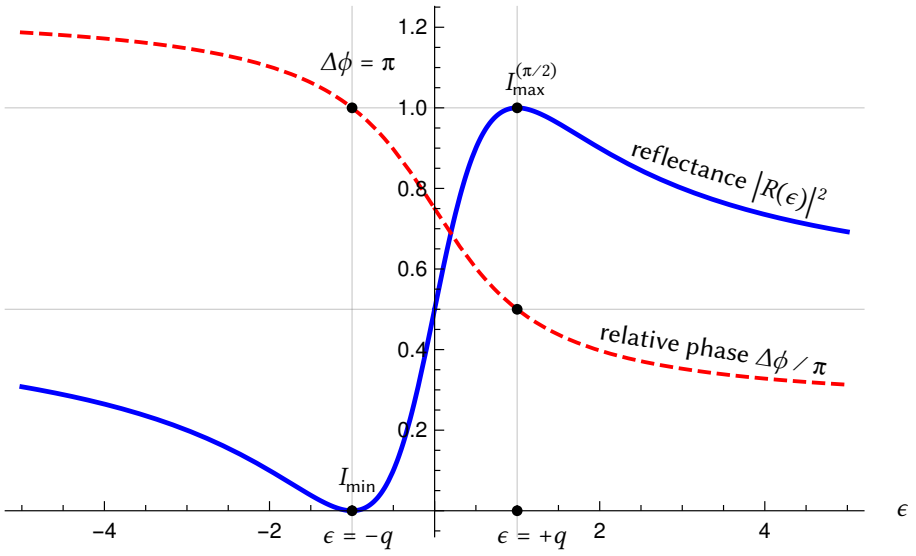

Figure 4.1: Fano line shape of the reflectance $|R_q(\epsilon)|^2$ (4.6) of the nuclear cavity system (blue) and the relative phase of the interfering channels (red dashed) in units of π for Fano parameter $q = 1$ and proportionality $a_0 = 1$. The horizontal axis is the energy detuning ϵ. For $\epsilon = -q$, total destructive interference occurs for a Fano line with real q. Then, the relative phase is $\Delta\phi = \pi$ (red line) for a relative minus sign between the amplitudes r_{cav} and r_{nuc}. The Fano maximum is at $\epsilon = 1 / q$, here $\epsilon = -1$, and does *not* correspond to a relative phase of zero but a finite phase; for this choice of $q = 1$, $\Delta\phi = \pi / 2$. The maximum of the spectrum occurs due to the $1 / \epsilon^2$ decay of the cavity amplitude r_{cav} in combination with the interference. The two points $+\epsilon and - \epsilon$ have equal amplitudes $rnuc$ and can thus be used to obtain an interference visibility (r_{cav} is constant for constant q). The choice $q = 1$ allows to choose $\epsilon = \pm 1$ and thus maximum and minimum, yielding maximal interference visibility.

$\epsilon = +1$ is the maximum, yielding the optimal visibility. This Fanop maximum has a relative phase of $\Delta\phi = \pi/2$ instead of a pure interference maximum with $\Delta\phi = 0$, so the standard textbook relation between $|g^{(1)}|$ and the visibility does not hold. We define the analog visibility $\mathrm{VIS}^{(\pi/2)}$ for our case where the minimum is at $\Delta\phi = \pi$ and the maximum is at $\Delta\phi = \pi \,/\, 2$:

$$\mathrm{VIS}^{(\pi/2)} = \frac{I_{\max}^{(\pi/2)} - I_{\min}}{I_{\max}^{(\pi/2)} + I_{\min}} \tag{4.8}$$

with

$$I_{\max}^{(\pi/2)} = I_{\mathrm{A}} + I_{\mathrm{B}} \quad \text{and} \tag{4.9}$$

$$I_{\min} = I_{\mathrm{A}} + I_{\mathrm{B}} - 2|\langle a^{\dagger} b\rangle| \,, \tag{4.10}$$

where I_{A} and I_{B} are the intensities of the interfering arms, correspondig to r_{nuc}^2 and r_{cav}^2. The visibility can be calculated, using the definition of $g^{(1)}$ (2.41), to the following relation:

$$\mathrm{VIS}^{(\pi/2)} = \frac{1}{\frac{2}{\chi\,|g^{(1)}|} - 1} \tag{4.11}$$

with

$$\chi = \frac{2\sqrt{I_{\mathrm{A}} I_{\mathrm{B}}}}{I_{\mathrm{A}} + I_{\mathrm{B}}} \leq 1 \,, \tag{4.12}$$

where as before, $\chi = 1$ for $I_{\mathrm{A}} = I_{\mathrm{B}}$. For our choice of $\epsilon = \pm 1$, $q = 1$ the amplitudes are equal and thus $\chi = 1$. Then,

$$|g^{(1)}| = \frac{2}{1 + \frac{1}{\mathrm{VIS}^{(\pi/2)}}} \tag{4.13}$$

$$\geq \mathrm{VIS}^{(\pi/2)} \tag{4.14}$$

so we can calculate $|g^{(1)}|$ from the interference visibility of the Fano line at $q = 1$ and $\epsilon = \pm 1$. This visibility is always greater than $|g^{(1)}|$ for $|g^{(1)}| \in (0, 1)$. For example, a visibility of $1 \,/\, 2$ yields $|g^{(1)}| = 2 \,/\, 3$.
Equivalently to the choice $q = 1$ and $\epsilon = \pm 1$, one can choose $q = -1$ and $\epsilon = \mp 1$.

Experimental Scheme

Experimentally, small deviations from $|q| = 1$ cannot be ruled out. Therefore, we propose the following procedure:
Record spectra and fit Fano curves to the experimental data to come as close to $q = 1$ as possible. Then extract $I_{\min}$ at $\epsilon = -q$ and ${I_{\max}}^{(\pi/2)}$ at $\epsilon = q$ to ensure $\chi = 1$. It can be easily verified that this procedure can only underestimate the

visibility, since $R(\epsilon = -q)$ is not the maximum for $q \neq 1$.
The relation (4.11) only holds for $\Delta\phi = \pi \nearrow 2$ at the maximum. For a deviation, $\Delta\phi = \pi \nearrow 2 - \delta$, we get

$$I_{\max}^{(\pi/2-\delta)} = I_A + I_B + 2\Delta|\langle a^\dagger b\rangle| \,, \tag{4.15}$$

with $\Delta = \cos(\pi \nearrow 2 - \delta)$. We can accordingly calculate the visibility

$$\mathrm{VIS}^{(\pi/2-\delta)} = \frac{1+\Delta}{\frac{2}{\chi\,|g^{(1)}|} - (1-\Delta)} \,, \tag{4.16}$$

which holds for all Δ, not just small values[1].While χ is still unity, Δ can be calculated from the fitted value of q, since for $\epsilon = q$, the relative phase is

$$\Delta\phi = \pi \nearrow 2 - \delta = 2\arctan\left(\frac{1}{q}\right) \,. \tag{4.17}$$

By this method, the exact value of $|g^{(1)}|$ can be obtained.

Evaluating Experimental Data

This procedure has been applied to Fano curve fits of experimental data of Ref. [Hee+15b], kindly provided by K. P. Heeg. The assumption of strong superradiance is satisfied in this data, while the deep-reflectivity-minimum is only approximately satisfied in these experiments. The Fano line shape for an incidence angle of $\Delta\theta = 29$ µrad from the cavity minimum can be seen in Ref. [Hee+15b], Fig. 2, lower left panel. This corresponds to $q = -0.94$. The modified interference visibility, obtained from the procedure explained above, is VIS = 0.50. Using (4.16), one obtains $|g^{(1)}| = 0.68$, very close to the minimum requirement $|g^{(1)}| \geq 0.707$.
A different cavity sample, reported in [Hee14] (cavity 1 in Fig. 4.2 (a), p. 42), shows better values: For $\Delta\theta = 30$ µrad, which corresponds to $q = -0.918$, the visibility is determined to VIS = 0.531, yielding $|g^{(1)}| = 0.712 > 0.707$ and thus a slightly larger value than minimally required for the Johansen criterion. Since not all assumptions are well satisfied for these two cavities, $|g^{(1)}|$ is not significantly greater than 0.707.
As discussed, higher values of $|g^{(1)}|$ are desirable. The limiting factor for the visibility is the baseline, which raises $I_{\min}$ to finite values. This baseline can be much lower for different cavity parameters. It is governed by two main factors: the depth of the empty cavity's reflectance minimum in the 'rocking curve', and by photons that do not scatter off the analyzer foil and are not excluded by the time-gating [2].

[1] For $\delta = \pi \nearrow 2$, i.e. $\Delta = 1$, the usual VIS = $|g^{(1)}|\,\chi$ is obtained.

[2] A detailed description of the experimental technique can be found in [Hee+15c], the supplemental material to [Hee+15b]

In [Rö+10], the empty cavity minimum (Fig. 1 B, ibid.) is very deep, satisfying our assumption, and the baseline is much smaller than the resonance line peak (Fig. 3 ibid., sample 1). R. Röhlsberger kindly provided the raw data for Fig. 3. A small baseline was subtracted in these spectra but even in the raw data, the contrast is very high due to the structural quality of the cavity [Rö17]. An interferometric visibility of >0.75 should be possible with such a cavity, and thus $|g^{(1)}| > 0.85$, well above the minimum requirement $|g^{(1)}| > 0.707$ for the Johansen criterion.

Discussion

We have solved here the problem of extracting the coherence $g^{(1)}$ for Fano interference. Theoretically, the formalism yields $|g^{(1)}| = 1$ because we get total destructive interference at $\epsilon = -q$ and thus VIS = 1. We addressed the experimental reality of a baseline by choosing optimal parameters, utilizing the maximum for $q = 1$. The practical difficulty of obtaining a Fano spectrum with $q = 1$ was solved by the experimental scheme that allowed arbitrary values of q. Investigating experimental data, we have shown that the thin-film cavity system is in principle capable of sufficiently high coherence. However, the peculiarities of the system require further careful analysis. Current experiments use broadband synchrotron pulses (compared to the nuclear resonance) and therefore have to exclude this prompt pulse from data analysis. One would need to examine whether the current experiments' results can be transferred to experiments with a single-photon source. Furthermore, the two interfering pathways both comprise multiple reflections in the cavity. One should carefully examine whether this has implications for the entanglement criterion, which is derived from a two-partite Bell test.
Experimentally, present cavities already provide good interferometric visibility. Further improvements are still desirable, because higher values of $|g^{(1)}|$ imply more robustness toward non-ideal values of $g^{(2)}$ for the Johansen criterion.

Experimental Outlook

While beamsplitters and interferometers are available for at least some portions of the hard x-ray spectrum, the biggest experimental challenge is to generate entangled states with a sufficient rate. Since parametric down-conversion is an established experimental technique in the visible spectrum, x-ray PDC is the most conservative approach to generate single-photon states that can subsequently be directed onto a beamsplitter for generating an entangled single-photon state. The discussed thin-film cavity system is at a disadvantage here, because it requires x-rays close to the neV-narrow nuclear resonance while beamsplitters are available for more photon energies. The availability of xPDC is therefore less likely for a nuclear system. It seems that the most likely realization of the full Johansen criterion is to use xPDC and a single-crystal interferometer, both of which have been used in x-ray experiments for years.

Furthermore, the crystal interferometer provides a means to test less established proposals such as the single-photon entanglement by coherent control of nuclear forward scattering [PKE09] [LP14]. Even testing only one of either $g^{(1)}$ or $g^{(2)}$ could provide meaningful insights on the physics involved.

Chapter 5

Summary & Outlook

In this thesis, an entanglement criterion for two spatial modes of light was investigated for its applicability in the hard x-ray regime. The criterion, put forward by Johansen [Joh96], is derived from a Bell inequality and can be tested by measuring the coherences $g^{(1)}$ by interferometry and $g^{(2)}$ in a coincidence experiment. The archetypal entanglement that can be detected by this criterion is the single-photon entangled state, which arises from a single photon impinging on a beamsplitter.

Employing a beamsplitter loss model in chapter 3, we investigated the effect of independent, finite losses in the two modes. We found that one obtains the same result for the criterion in both the lossless and the lossy case, making the criterion robust against losses in an experimental implementation.
We investigated a general beamsplitter, illuminated by a single mode, as a possible source for entanglement and showed that the criterion is also independent of the beamsplitter reflectance. We presented the resulting criterion for the single-mode input and showed that the beamsplitter reduces the criterion to a coincidence criterion. Furthermore, the remaining criterion can be formulated in the intuitive quantities of photon statistics; mean photon number and variance in photon number. Meeting the criterion implies sub-Poissonian statistics of the input state. The single-mode criterion is perfectly met for any mixture of the single-photon state and the vacuum. Furthermore, a single-photon input state with arbitrary admixtures, if sufficiently small, were shown to meet the criterion as well. Thus, the criterion does not need an idealized single-photon input, making it practical for experimental implementation.

In order to grasp the criterion's power and its limitations, we investigated a wide range of states for the beamsplitter input in section 3.3. States close to the single-photon were shown to generate an entangled state. We investigated different states that meet a more general criterion: the full Bell inequality from which the Johansen criterion is derived. We illustrated that there are forms of entanglement that cannot be detected by the Johansen criterion but by the full Bell criterion,

such as the squeezed vacuum state. This state is considerably different from the single-photon state as it may produce one photon in each arm after impinging on the beamsplitter.
We investigated a coherent state input in order to illustrate the difference between weak classical states and a single-photon state. While a coherent state of arbitrary parameter α will always produce a separable, i.e. non-entangled state, an at–most–one–photon input will form entanglement. Thus, approximating a weak coherent state with at most to one photon distorts the result of the criterion drastically. This discussion is not new in quantum theory, but appears to receive too little attention in the field of nuclear x-ray optics. It has important implications for both the generation and the verification of single-photon entanglement under the usual condition of very low count rates [Ada03] [HT99].
While the previous discussion was based on the input states, we implemented a post-selection calculation in section 3.4 to investigate the effect of discarding events after the experiments. It shows that discarding certain events changes the obtained results drastically. We showed that post-selecting events with *at most one* photon detection always yields 'entanglement criterion met' for arbitrary input states, even the coherent state. Post-selecting events with *at least one* photon detection changes the coherent state's result to 'entanglement criterion met' for a wide range of parameters.
The approximation of a weak coherent state with *at most* two photons (truncating) was shown not to change the result of the entanglement test. It is therefore crucial for both experiment and theory not to neglect two-photon events in the context of this criterion, no matter how infrequent their occurrence.

Because of experimental limitations, an easier criterion would be of great interest. We reviewed Lee and Kim's proposal for a single-photon Bell inequality that uses only a Mach-Zehnder interferometer in section 3.5. We showed that the prerequisites of the inequality demand an ideal, entangled state. This makes it impossible to use it for entanglement detection. We argued further that the underlying reasoning is unconvincing due to its questionable notion of locality in an interference setup.

The encouraging theoretical results about the robustness of Johansen's criterion motivated a look into currently available x-ray technology in chapter4. The robustness towards losses circumvents many experimental problems. We found that the beamsplitter and interferometer technology is well advanced and should be capable of implementing the criterion. Constructing an entanglement source remains a challenge because of the low production rate of x-ray parametric down-conversion in this energy regime. We suggested using a monolithic crystal interferometer to measure both the interference and coincidence at once, using the low xPDC rate efficiently.
Proposals for single-photon entanglement generation with nuclear forward scattering were discussed. While the results of this thesis do not allow to draw conclu-

sions about these systems, the discussed difference between weak classical states and single-photon states motivates further theoretical and experimental investigation of these proposals.
In section 4.3, Mössbauer nuclei in thin-film cavities were investigated in more detail. Using the interpretation of the system as a two-arm interferometer, we demonstrated that the Fano interference differs from Mach-Zehnder interference: Due to simultaneously varying phase and amplitude of the interfering channels and a limited range of the relative phase, maxima of Fano curves do not correspond to maximal interference. We derived a relation between interference visibility and $g^{(1)}$, special for the Fano interference case. Choosing the optimal Fano parameter, we showed that the system is in theory capable of full coherence $|g^{(1)}| = 1$.
In order to investigate the coherence in experiment, we put forward an procedure to extract $|g^{(1)}|$ from Fano lines of arbitrary Fano parameter q. Analyzing experimental data, we showed that the cavity is capable of sufficiently high values of $|g^{(1)}|$ for the entanglement criterion.

The presented derivation of the Johansen criterion and its practicability shows that it can be worth it to take a step back from current experimental limitations: The starting point of the discussed criterion is a Bell experiment using local oscillators, which is clearly beyond today's x-ray technology. However, the final criterion can be checked with only beamsplitters and detectors, well within reach for current experiments.

Outlook

Deriving an entanglement criterion from a Bell inequality is not limited to this specific Bell inequality. Applying the method to a different Bell inequality might yield a new and useful criterion. It could be sensitive to different entangled states, increasing the total range of detectable entangled states. For example, [Che+02] showed how to transfer the Bell–CHSH inequality from discrete to continuous variable measurements in a general way. A number of parameters can be chosen freely in this scheme, so one may be able to derive a different entanglement criterion by an analogue calculation. The Bell inequality itself does not need to be experimentally simple in order to derive a practical criterion.

Our investigation of nuclei in thin-film cavities may guide the construction of cavities optimized for high coherence. Aside from the entanglement criterion, a cavity of high coherence may enhance the system's sensitivity for the multitude of envisaged precision metrology applications [Hee+15b].
On the theory side of the cavity systems, an examination of the process with a single photon is an interesting research direction. While the Johansen criterion would be fulfilled for a single-photon input, it is interesting to investigate what

type of entanglement would be produced in the system and whether it could be used to exploit other quantum effects.

While the Johansen criterion is derived from, but not equivalent to a proper Bell test, it is a useful first step. It allows to solve the problem of reliable entanglement production at x-ray energies independent from the problem of performing Bell measurements with local oscillators. However, the rapid improvements in x-ray technology and especially x-ray quantum optics will enable more elaborate experiments in the future. One of the biggest such endeavours is the design and construction of a x-ray free electron laser oscillator (XFELO) [KSR08] that would yet again push the limits of coherence properties of x-ray light sources. An XFELO may enable the x-ray quantum optics community to perform a local oscillator Bell experiment, testing nature's fundamental principles in this new energy regime.

Bibliography

[Ada03] B. W. Adams.
Nonlinear Optics, Quantum Optics, and Ultrafast Phenomena with X-Rays.
Springer Science+Business Media New York, 2003.
ISBN: 978-1-4613-5051-4.
URL: http://www.springer.com/gp/book/9781402074752 (visited on 08/07/2017).

[Alt+06] M. Altarelli et al.
"The European x-ray free-electron laser".
In: *Technical Design Report, DESY* 97 (2006), pp. 1–26.

[BB84] C. H. Bennett and G. Brassard.
"Quantum cryptography: Public key distribution and coin tossing".
In: *Theoretical Computer Science*. Theoretical Aspects of Quantum Cryptography – celebrating 30 years of BB84 560 (1984), pp. 7–11.
ISSN: 0304-3975.
DOI: 10.1016/j.tcs.2014.05.025.

[Bel64] J. S. Bell.
"On the Einstein Podolsky Rosen paradox".
In: *Physics* 1 (1964), pp. 195–200.

[BEW05] D. H. Bilderback, P. Elleaume, and E. Weckert.
"Review of third and next generation synchrotron light sources". en.
In: *Journal of Physics B: Atomic, Molecular and Optical Physics* 38.9 (2005), S773.
ISSN: 0953-4075.
DOI: 10.1088/0953-4075/38/9/022.

[Bey+13] M. Beye et al.
"Stimulated X-ray emission for materials science".
In: *Nature* 501.7466 (Sept. 2013), pp. 191–194.
ISSN: 0028-0836.
URL: http://dx.doi.org/10.1038/nature12449.

[BG77] U. Bonse and W. Graeff.
"X-ray and neutron interferometry". en.
In: *X-Ray Optics*.
Topics in Applied Physics.
DOI: 10.1007/3-540-08462-2_10.
Springer, Berlin, Heidelberg, 1977,
Pp. 93–143.
ISBN: 978-3-540-08462-4 978-3-540-37042-0.
URL: https://link.springer.com/chapter/10.1007/3-540-08462-2_10 (visited on 08/17/2017).

[BH65] U. Bonse and M. Hart.
"An x-ray interferometer".
In: *Applied Physics Letters* 6.8 (Apr. 1965), pp. 155–156.
ISSN: 0003-6951.
DOI: 10.1063/1.1754212.

[BKS97] H. Beyer, H.-J. Kluge, and V. Shevelko.
X-Ray Radiation of Highly Charged Ions.
Springer Berlin Heidelberg, 1997.
URL: http://www.springer.com/de/book/9783540631859 (visited on 08/14/2017).

[Bus02] J. T. Bushberg.
The essential physics of medical imaging.
Lippincott Williams & Wilkins, 2002.
ISBN: 0-683-30118-7.

[Car+01] J. J. Carroll et al.
"X-Ray-Driven Gamma Emission".
In: *Hyperfine Interactions* 135.1 (July 2001), pp. 3–50.
ISSN: 1572-9540.
DOI: 10.1023/A:1013967219408.

[Che+02] Z.-B. Chen et al.
"Maximal Violation of Bell's Inequalities for Continuous Variable Systems".
In: *Physical Review Letters* 88.4 (Jan. 2002), p. 040406.
DOI: 10.1103/PhysRevLett.88.040406.

[Cir80] B. S. Cirel'son.
"Quantum generalizations of Bell's inequality". en.
In: *Letters in Mathematical Physics* 4.2 (Mar. 1980), pp. 93–100.
ISSN: 0377-9017, 1573-0530.
DOI: 10.1007/BF00417500.

[Cla+69] J. F. Clauser et al.
"Proposed Experiment to Test Local Hidden-Variable Theories".
In: *Physical Review Letters* 23.15 (Oct. 1969), pp. 880–884.
DOI: 10.1103/PhysRevLett.23.880.

[DiV95] D. P. DiVincenzo.
"Quantum Computation".
In: *Science* 270.5234 (Oct. 1995), p. 255.
DOI: 10.1126/science.270.5234.255.

[Dre07] J. Drenth.
Principles of Protein X-Ray Crystallography.
2007.
URL: http://www.springer.com/de/book/9780387333342
(visited on 08/13/2017).

[EB72] A. Einstein and M. Born.
Briefwechsel 1916–1955.
Rowohlt Taschenbuchverlag, 1972.
ISBN: 978-3-485-00633-0.

[EM71] P. Eisenberger and S. L. McCall.
"X-Ray Parametric Conversion".
In: *Physical Review Letters* 26.12 (Mar. 1971), pp. 684–688.
DOI: 10.1103/PhysRevLett.26.684.

[Emm+10] P. Emma et al.
"First lasing and operation of an ångstrom-wavelength free-electron laser". en.
In: *Nature Photonics* 4.9 (Sept. 2010), pp. 641–647.
ISSN: 1749-4885.
DOI: 10.1038/nphoton.2010.176.

[EPR35] A. Einstein, B. Podolsky, and N. Rosen.
"Can Quantum-Mechanical Description of Physical Reality Be Considered Complete?"
In: *Physical Review* 47.10 (May 1935), pp. 777–780.
DOI: 10.1103/PhysRev.47.777.

[FC72] S. J. Freedman and J. F. Clauser.
"Experimental Test of Local Hidden-Variable Theories".
In: *Physical Review Letters* 28.14 (Apr. 1972), pp. 938–941.
DOI: 10.1103/PhysRevLett.28.938.

[Fuw+15] M. Fuwa et al.
"Experimental proof of nonlocal wavefunction collapse for a single particle using homodyne measurements". en.
In: *Nature Communications* 6 (Mar. 2015), p. 6665.
DOI: 10.1038/ncomms7665.

[Gen05] M. Genovese.
"Research on hidden variable theories: A review of recent progresses".
In: *Physics Reports* 413.6 (July 2005), pp. 319–396.
ISSN: 0370-1573.
DOI: 10.1016/j.physrep.2005.03.003.

[GHZ95] D. M. Greenberger, M. A. Horne, and A. Zeilinger.
"Nonlocality of a Single Photon?"
In: *Physical Review Letters* 75.10 (Sept. 1995), pp. 2064–2064.
DOI: 10.1103/PhysRevLett.75.2064.

[Gis+02] N. Gisin et al.
"Quantum cryptography".
In: *Reviews of Modern Physics* 74.1 (Mar. 2002), pp. 145–195.
DOI: 10.1103/RevModPhys.74.145.

[Giu+15] M. Giustina et al.
"Significant-Loophole-Free Test of Bell's Theorem with Entangled Photons".
In: *Physical Review Letters* 115.25 (Dec. 2015), p. 250401.
DOI: 10.1103/PhysRevLett.115.250401.

[GK04] C. Gerry and P. Knight.
Introductory quantum optics.
Cambridge University Press, 2004.
ISBN: 978-0-521-52735-4.
URL: http://www.cambridge.org/de/academic/subjects/physics/optics-optoelectronics-and-photonics/introductory-quantum-optics.

[Glo+10] T. E. Glover et al.
"Controlling X-rays with light".
In: *Nat Phys* 6.1 (Jan. 2010), pp. 69–74.
ISSN: 1745-2473.
DOI: 10.1038/nphys1430.

[Glo+12] T. E. Glover et al.
"X-ray and optical wave mixing".
In: *Nature* 488.7413 (Aug. 2012), pp. 603–608.
ISSN: 0028-0836.
DOI: 10.1038/nature11340.

[Gra88] P. Grangier.
"Probing the phase coherence of parametrically generated photon pairs: A new test of Bell's inequalities".
In: *Physical Review A* 38.6 (1988), pp. 3132–3135.
DOI: 10.1103/PhysRevA.38.3132.

[GT09] O. Gühne and G. Tóth.
"Entanglement detection".
In: *Physics Reports* 474.1–6 (Apr. 2009), pp. 1–75.
ISSN: 0370-1573.
DOI: 10.1016/j.physrep.2009.02.004.

[Har94] L. Hardy.
"Nonlocality of a Single Photon Revisited".
In: *Physical Review Letters* 73.17 (Oct. 1994), pp. 2279–2283.
DOI: 10.1103/PhysRevLett.73.2279.

[HE13] K. P. Heeg and J. Evers.
"X-ray quantum optics with Mössbauer nuclei embedded in thin film cavities".
In: *Physical Review A* 88.4 (Oct. 2013). arXiv: 1305.4239.
ISSN: 1050-2947, 1094-1622.
DOI: 10.1103/PhysRevA.88.043828.

[Hee14] K. P. Heeg.
"X-Ray Quantum Optics With Mössbauer Nuclei In Thin-Film Cavities".
PhD thesis. Ruprecht-Karls-Universität Heidelberg, Dec. 2014.
URL: http://doi.org/10.11588/heidok.00017869.

[Hee+13] K. P. Heeg et al.
"Vacuum-Assisted Generation and Control of Atomic Coherences at X-Ray Energies".
In: *Physical Review Letters* 111.7 (Aug. 2013), p. 073601.
DOI: 10.1103/PhysRevLett.111.073601.

[Hee+15a] K. P. Heeg et al.
"Tunable sub-luminal propagation of narrowband x-ray pulses".
In: *Physical Review Letters* 114.20 (May 2015). arXiv: 1409.0365.
ISSN: 0031-9007, 1079-7114.
DOI: 10.1103/PhysRevLett.114.203601.

[Hee+15b] K. Heeg et al.
"Interferometric phase detection at x-ray energies via Fano resonance control".
In: *Physical Review Letters* 114.20 (May 2015), p. 207401.
DOI: 10.1103/PhysRevLett.114.207401.

[Hee+15c] K. Heeg et al.
"Supplemental Material to: Interferometric phase detection at x-ray energies via Fano resonance control".
In: *Physical Review Letters* 114.20 (May 2015), p. 207401.
URL: https://journals.aps.org/prl/supplemental/10.1103/PhysRevLett.114.207401 (visited on 08/11/2017).

[Hen+15] B. Hensen et al.
"Loophole-free Bell inequality violation using electron spins separated by 1.3 kilometres". en.
In: *Nature* 526.7575 (Oct. 2015), pp. 682–686.
ISSN: 0028-0836.
DOI: 10.1038/nature15759.

[Hes+04] B. Hessmo et al.
"Experimental Demonstration of Single Photon Nonlocality".
In: *Physical Review Letters* 92.18 (May 2004), p. 180401.
DOI: 10.1103/PhysRevLett.92.180401.

[HT99] J. Hannon and G. Trammell.
"Coherent ɣ-ray optics".
In: *Hyperfine Interactions* 123.1 (Mar. 1999), pp. 127–274.
ISSN: 1572-9540.
DOI: 10.1023/A:1017011621007.

[Jac07] J. D. Jackson.
Classical electrodynamics.
John Wiley & Sons, 2007.
ISBN: 81-265-1094-3.

[Joh96] L. M. Johansen.
"Bell's inequality for the Mach-Zehnder interferometer".
In: *Physics Letters A* 219.1 (Aug. 1996), pp. 15–18.
ISSN: 0375-9601.
DOI: 10.1016/0375-9601(96)00437-9.

[JW11] S. J. Jones and H. M. Wiseman.
"Nonlocality of a single photon: Paths to an Einstein-Podolsky-Rosen-steering experiment".
In: *Physical Review A* 84.1 (July 2011), p. 012110.
DOI: 10.1103/PhysRevA.84.012110.

[KLM01] E. Knill, R. Laflamme, and G. J. Milburn.
"A scheme for efficient quantum computation with linear optics". en.
In: *Nature* 409.6816 (Jan. 2001), pp. 46–52.
ISSN: 0028-0836.
DOI: 10.1038/35051009.

[KSR08] K.-J. Kim, Y. Shvyd'ko, and S. Reiche.
"A Proposal for an X-Ray Free-Electron Laser Oscillator with an Energy-Recovery Linac".
In: *Physical Review Letters* 100.24 (June 2008), p. 244802.
DOI: 10.1103/PhysRevLett.100.244802.

[Kun+97] Y. Kunimune et al.
"Two-Photon Correlations in X-rays from a Synchrotron Radiation Source". en.
In: *Journal of Synchrotron Radiation* 4.4 (July 1997), pp. 199–203.
ISSN: 0909-0495.
DOI: 10.1107/S0909049597006912.

[Lau14] F. Lauble.
"Erzeugung eines nuklearen Polaritons mit zwei verschränkten Zweigen mithilfe von Magnetfelddrehungen". German.
Bachelor Thesis. Heidelberg: Ruprecht-Karls-Universität Heidelberg, 2014.

[LK00] H.-W. Lee and J. Kim.
"Quantum teleportation and Bell's inequality using single-particle entanglement".
In: *Physical Review A* 63.1 (Dec. 2000), p. 012305.
DOI: 10.1103/PhysRevA.63.012305.

[LKP16] W.-T. Liao, C. H. Keitel, and A. Pálffy.
"X-ray-generated heralded macroscopical quantum entanglement of two nuclear ensembles".
In: *Scientific Reports* 6 (Sept. 2016), p. 33361.
ISSN: 2045-2322.
DOI: 10.1038/srep33361.

[Lom+02] E. Lombardi et al.
"Teleportation of a Vacuum–One-Photon Qubit".
In: *Physical Review Letters* 88.7 (Jan. 2002), p. 070402.
DOI: 10.1103/PhysRevLett.88.070402.

[LP14] W.-T. Liao and A. Pálffy.
"Proposed Entanglement of X-ray Nuclear Polaritons as a Potential Method for Probing Matter at the Subatomic Scale".
In: *Physical Review Letters* 112.5 (Feb. 2014), p. 057401.
DOI: 10.1103/PhysRevLett.112.057401.

[Mö58] R. L. Mössbauer.
"Kernresonanzfluoreszenz von Gammastrahlung in Ir191".
In: *Zeitschrift für Physik* 151.2 (Apr. 1958), pp. 124–143.
ISSN: 0044-3328.
DOI: 10.1007/BF01344210.

[Mun] R. Munroe.
xkcd: Bell's Theorem.
URL: https://xkcd.com/1591/ (visited on 08/19/2017).

[NC02] M. A. Nielsen and I. Chuang.
"Quantum Computation and Quantum Information".
In: *American Journal of Physics* 70.5 (Apr. 2002), pp. 558–559.
ISSN: 0002-9505.
DOI: 10.1119/1.1463744.

[OS89] B. J. Oliver and C. R. Stroud.
"Predictions of violations of Bell's inequality in an 8-port homodyne detector".
In: *Physics Letters A* 135.8 (Mar. 1989), pp. 407–410.
ISSN: 0375-9601.
DOI: 10.1016/0375-9601(89)90036-4.

[Osa+13] T. Osaka et al.
"A Bragg beam splitter for hard x-ray free-electron lasers". EN.
In: *Optics Express* 21.3 (Feb. 2013), pp. 2823–2831.
ISSN: 1094-4087.
DOI: 10.1364/OE.21.002823.

[Pel+16] D. Pelliccia et al.
"Experimental X-Ray Ghost Imaging".
In: *Physical Review Letters* 117.11 (Sept. 2016), p. 113902.
DOI: 10.1103/PhysRevLett.117.113902.

[Per02] A. Peres.
Quantum Theory: Concepts and Methods.
2002.
ISBN: 978-0-7923-2549-9.
URL: http://www.springer.com/gp/book/9780792325499
(visited on 08/06/2017).

[Per95] A. Peres.
"Nonlocal Effects in Fock Space".
In: *Physical Review Letters* 74.23 (June 1995), pp. 4571–4571.
DOI: 10.1103/PhysRevLett.74.4571.

[PKE09] A. Pálffy, C. H. Keitel, and J. Evers.
"Single-Photon Entanglement in the keV Regime via Coherent Control of Nuclear Forward Scattering".
In: *Physical Review Letters* 103.1 (July 2009), p. 017401.
DOI: 10.1103/PhysRevLett.103.017401.

[PT04] A. Peres and D. R. Terno.
"Quantum information and relativity theory".
In: *Reviews of Modern Physics* 76.1 (Jan. 2004), pp. 93–123.
DOI: 10.1103/RevModPhys.76.93.

[Rö17] R. Röhlsberger.
In: *Private Communication* (2017).

[Rö98] W. C. Röntgen.
"Ueber eine neue Art von Strahlen". en.
In: *Annalen der Physik* 300.1 (Jan. 1898), pp. 1–11.
ISSN: 1521-3889.
DOI: 10.1002/andp.18983000102.

[Rö+10] R. Röhlsberger et al.
"Collective Lamb Shift in Single-Photon Superradiance". en.
In: *Science* 328.5983 (June 2010), pp. 1248–1251.
ISSN: 0036-8075, 1095-9203.
DOI: 10.1126/science.1187770.

[Rö+12] R. Röhlsberger et al.
"Electromagnetically induced transparency with resonant nuclei in a cavity".
In: *Nature* 482.7384 (Feb. 2012), pp. 199–203.
ISSN: 0028-0836.
DOI: 10.1038/nature10741.

[Roh+12] N. Rohringer et al.
"Atomic inner-shell X-ray laser at 1.46 nanometres pumped by an X-ray free-electron laser".
In: *Nature* 481.7382 (Jan. 2012), pp. 488–491.
ISSN: 0028-0836.
DOI: 10.1038/nature10721.

[RW86] M. D. Reid and D. F. Walls.
"Violations of classical inequalities in quantum optics".
In: *Physical Review A* 34.2 (Aug. 1986), pp. 1260–1276.
DOI: 10.1103/PhysRevA.34.1260.

[San92a] E. Santos.
"Comment on "Nonlocality of a single photon"".
In: *Physical Review Letters* 68.6 (Feb. 1992), pp. 894–894.
DOI: 10.1103/PhysRevLett.68.894.

[San92b] E. Santos.
"Santos replies".
In: *Physical Review Letters* 68.17 (Apr. 1992), pp. 2702–2703.
DOI: 10.1103/PhysRevLett.68.2702.

[SH11] S. Shwartz and S. E. Harris.
"Polarization Entangled Photons at X-Ray Energies".
In: *Physical Review Letters* 106.8 (Feb. 2011), p. 080501.
DOI: 10.1103/PhysRevLett.106.080501.

[Sha+15] L. K. Shalm et al.
"Strong Loophole-Free Test of Local Realism".
In: *Physical Review Letters* 115.25 (Dec. 2015), p. 250402.
DOI: 10.1103/PhysRevLett.115.250402.

[Shi03] Y. Shih.
"Entangled biphoton source - property and preparation". en.
In: *Reports on Progress in Physics* 66.6 (2003), p. 1009.
ISSN: 0034-4885.
DOI: 10.1088/0034-4885/66/6/203.

[Shv+96] Y. V. Shvyd'ko et al.
"Storage of Nuclear Excitation Energy through Magnetic Switching".
In: *Physical Review Letters* 77.15 (Oct. 1996), pp. 3232–3235.
DOI: 10.1103/PhysRevLett.77.3232.

[Shw+14] S. Shwartz et al.
"X-Ray Second Harmonic Generation".
In: *Physical Review Letters* 112.16 (Apr. 2014), p. 163901.
DOI: 10.1103/PhysRevLett.112.163901.

[Tam+11] K. Tamasaku et al.
"Visualizing the local optical response to extreme-ultraviolet radiation with a resolution of λ/380". en.
In: *Nature Physics* 7.9 (Sept. 2011), pp. 705–708.
ISSN: 1745-2473.
DOI: 10.1038/nphys2044.

[TG65] U. M. Titulaer and R. J. Glauber.
"Correlation Functions for Coherent Fields".
In: *Physical Review* 140.3B (Nov. 1965), B676–B682.
DOI: 10.1103/PhysRev.140.B676.

[THW90] S. M. Tan, M. J. Holland, and D. F. Walls.
"Bell's inequality for systems with quadrature phase coherence".
In: *Optics Communications* 77.4 (July 1990), pp. 285–291.
ISSN: 0030-4018.
DOI: 10.1016/0030-4018(90)90092-8.

[TI07] K. Tamasaku and T. Ishikawa.
"Interference between Compton Scattering and X-Ray Parametric Down-Conversion".
In: *Physical Review Letters* 98.24 (June 2007), p. 244801.
DOI: 10.1103/PhysRevLett.98.244801.

[TWC91] S. M. Tan, D. F. Walls, and M. J. Collett.
"Nonlocality of a single photon".
In: *Physical Review Letters* 66.3 (Jan. 1991), pp. 252–255.
DOI: 10.1103/PhysRevLett.66.252.

[TWC92] S. M. Tan, D. F. Walls, and M. J. Collett.
"Tan, Walls, and Collett reply".
In: *Physical Review Letters* 68.6 (Feb. 1992), pp. 895–895.
DOI: 10.1103/PhysRevLett.68.895.

[TYI02] K. Tamasaku, M. Yabashi, and T. Ishikawa.
"X-Ray Interferometry with Multicrystal Components Using Intensity Correlation".
In: *Physical Review Letters* 88.4 (Jan. 2002), p. 044801.
DOI: 10.1103/PhysRevLett.88.044801.

[War69] B. E. Warren.
X-Ray Diffraction.
Addison-Wesley, 1969.

[WM94] D. F. Walls and G. J. Milburn.
Quantum optics.
1st ed.
Springer-Verlag Berlin Heidelberg, 1994.
ISBN: 978-7-5062-3627-0.

[Yon+15] H. Yoneda et al.
"Atomic inner-shell laser at 1.5-angstrom wavelength pumped by an X-ray free-electron laser". en.
In: *Nature* 524.7566 (Aug. 2015), pp. 446–449.
ISSN: 0028-0836.
DOI: 10.1038/nature14894.

[Zha16] L. Zhang.
In: *Private Communication* (2016).

[Mik07] Mikm.
The EPR thought experiment (as seen in Sakurai's Bell inequality).
Jan. 2007.
URL: https://commons.wikimedia.org/wiki/File:EPR_thought_experiment.svg (visited on 08/18/2017).

Acknowledgements

Mein großer Dank geht an meinen Betreuer Jörg Evers, der sich immer genügend Zeit für Besprechungen und Diskussionen mit mir nahm. Ich danke für die Chance an diesem spannenden Projekt zu arbeiten und dafür, dass er offen für meine Ideen und Vorschläge war.
Ich möchte Zoltán Harman dafür danken, dass er sich bereit erklärt hat, die Zweitbegutachtung dieser Arbeit zu übernehmen.
Über das Projekt wurde ich von Kilian Heeg in großem Maße unterstützt. Insbesondere für die zahlreichen Antworten auf meine Fragen zu den Cavity-Systemen und seine großartige Arbeit beim Korrekturlesen möchte ich mich herzlich bedanken.
Korrektur gelesen haben diese Arbeit ebenfalls Dominik, Jascha, Hannah, Hendrik, Micha und Nadia, wofür ihnen mein Dank gebührt. Dominik tat sich mit der Bereitschaft für Korrekturen in letzter Minute dabei besonders hervor. ;-)
Sämtliche Fehler in der Arbeit sind selbstverständlich meine eigenen und sind den KorrekturleserInnen nicht anzulasten.
Für die Gelegenheit, bei einem Experiment am DESY teilzunehmen, möchte ich mich bei Jörg und Professor Keitel herzlich bedanken.
Ralf Röhlsberger möchte ich dafür danken, dass er mir so schnell und hilfsbereit antwortete und seine experimentellen Rohdaten zur Verfügung stellte.
I would like to thank my colleagues for the pleasant time at the institute. Dominik, Jörg, Kilian, Lida, Naveen, Salvatore and Stefano deserve special mention for the joyful office atmosphere, lunch breaks or coffee partys I shared with them.

Meinen besonderen Dank verdienen jene, die mich während meines Studiums und dieser Masterarbeit begleitet haben. Auf diese Menschen, die viele kleine und einige große Dinge leisteten, hätte ich nicht verzichten können.

Erklärung:

Ich versichere, dass ich diese Arbeit selbständig verfasst und keine anderen als die angegebenen Quellen und Hilfsmittel benutzt habe.

Heidelberg, 23. August 2017 .....

Fabian Lauble